

**Figure 2. Canonical and noncanonical pathways of NF- $\kappa$ B signaling are activated in AML1-deficient cells.** (A) Immunofluorescent staining of p65 in c-kit + BM cells transduced with CreER or mock from AML1 flox/flox (f/f) mice with or without BMS-345541 (1  $\mu$ M). Scale bar represents 10  $\mu$ m. Blue indicates TO-PRO3 (nucleus), and red indicates p65. The mean intensity of nuclear localized p65 was quantified with ImageJ Version 1.41o software.<sup>31</sup> (B) Fractionated Western blotting of p65 in c-kit + BM cells of AML1-deficient (AML1 f/f Mx+), or control (AML1 f/f Mx-) mice. (C) NFKB2 mRNA expression in BM cells transduced with CreER or mock from AML1 f/f mice 48 hours after 4-OHT addition. Error bars show mean  $\pm$  SEM (D) Western blotting of NFKB2 (p100 or p52) in B220 + spleen cells from AML1 cKO mice (AML1 f/f Mx+) or control mice (AML1 f/f Mx-) with or without BAFF (200 ng/mL). Protein levels were quantified with ImageJ Version 1.41o software.<sup>31</sup>

AML1 results in the inhibition of both nuclear translocation of p65 and activation of NF- $\kappa$ B target genes.

#### Critical role for NF- $\kappa$ B signaling in the myeloid transformation induced by AML1 mutants

Next, we analyzed the contribution of NF- $\kappa$ B signaling to AML1-related myeloid transformation. We found that 3 types of AML1 mutants, A224fsX228, S291fsX300, and R293X, can transform bone marrow cells in a serial replating assay (Figure 5A and supplemental Figure 2A). A224fsX228 and S291fsX300

were found in human cases with MDS. Similar types of mutants, N209fsX233, R290fsX299, and V292fsX300, were found in cases with de novo AML. R293X was found in both cases with MDS and de novo AML. These mutants belong to the C-terminally truncated type.<sup>3,5,40</sup> Among these mutants, it was recently reported that S291fsX300 induce AML in a mouse BMT model, indicating the in vivo transforming activity of this mutant.<sup>13</sup> We first assessed the effect of S291fsX300 overexpression on NF- $\kappa$ B signaling. Remarkably, in contrast to the wild type of AML1, S291fsX300 did not inhibit p65 nuclear

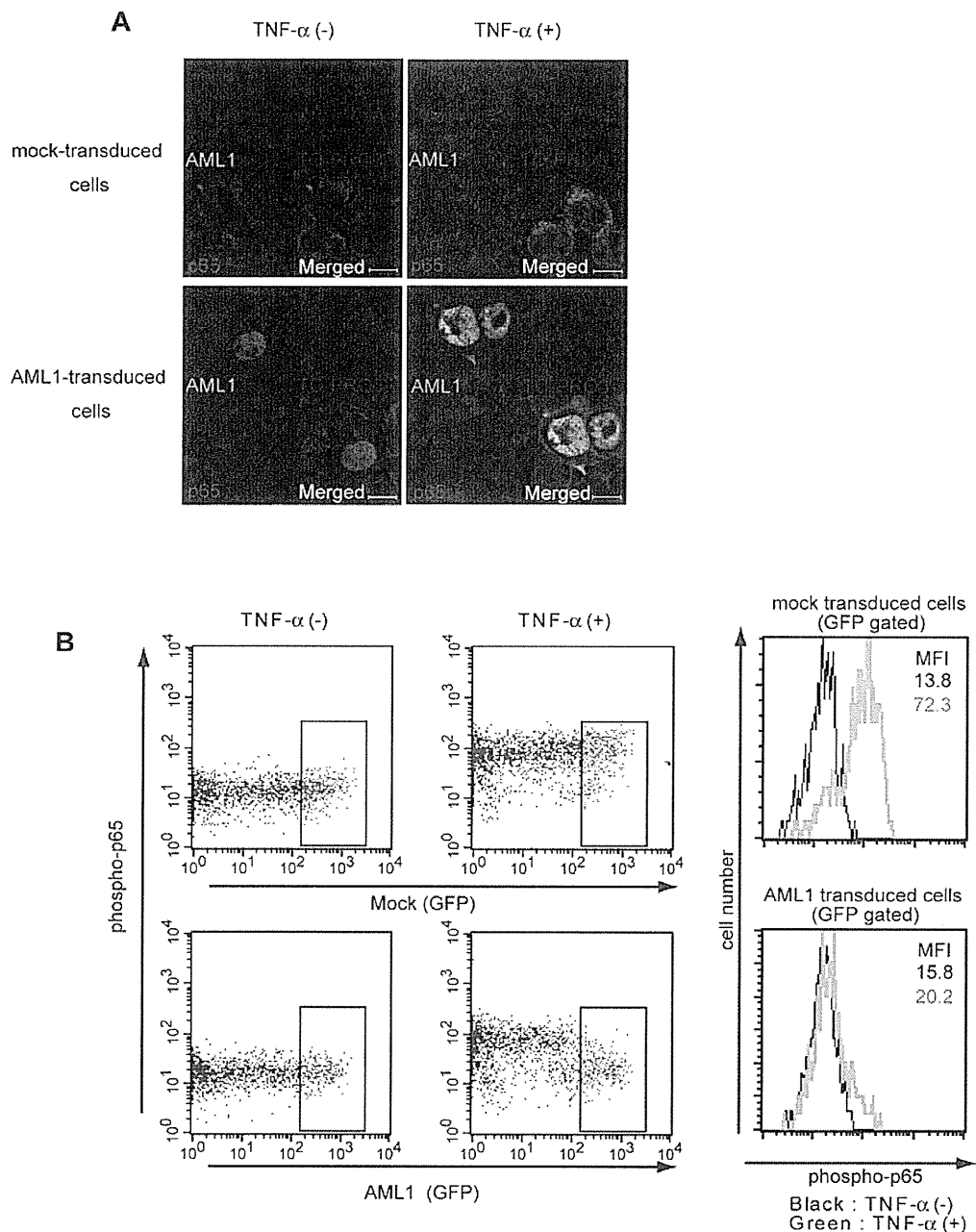


**Figure 3. AML1 inhibits nuclear translocation and phosphorylation of p65.** (A) Nuclear translocation assays of p65 in HEK293T cells transduced with AML1 or mock, 20 minutes after the addition of TNF- $\alpha$ . Scale bar represents 10  $\mu$ m. Green indicates AML1; blue indicates TO-PRO3 (nucleus); and red indicates p65. (B) Intracellular FACS analysis of phospho-p65 (Ser 536) in HEK293T cells transduced with AML1 or mock. GFP-positive fractions were gated. Green line shows phosphorylated p65 protein 5 minutes after TNF- $\alpha$  stimulation. MFI indicates mean fluorescence intensity.

translocation induced by TNF- $\alpha$  (Figure 5B-C). As is compatible with these findings, S291fsX300 has lost the ability to repress kinase activities of IKK $\alpha$  and IKK $\beta$  (Figure 5D-E). In addition, neither A224fsX228 nor R293X inhibited p65 nuclear translocation (Figure 5F-G). In accordance with the inability to inhibit NF- $\kappa$ B signaling, replating capacity of the bone marrow cells introduced with these 3 mutants was highly susceptible to the pharmacologic inhibition of NF- $\kappa$ B signaling by BMS-345541 (Figure 5H). In-frame mutation in the Runt domain such as D171N is another type of AML1 abnormality frequently found in MDS patients (supplemental Figure 2B).<sup>12</sup> We found that D171N also did not inhibit p65 nuclear translocation

(supplemental Figure 2C). Consistently, the inhibitory effect against IKK activity of D171N was attenuated (supplemental Figure 2D-E). These results suggest that the loss of inhibition of NF- $\kappa$ B signaling is a critical mechanism shared by many types of AML1 mutants in the development of AML.

To seek the NF- $\kappa$ B inhibitory domain of AML1, we analyzed a series of deletion mutants of AML1 in nuclear translocation assays of p65 (supplemental Figure 3A). As shown in supplemental Figure 3B, AML1  $\Delta$ 444, which lacks the domain interacting with a corepressor TLE, inhibited p65 nuclear translocation, whereas AML1  $\Delta$ 335, AML1a, a truncated isoform of AML1, or AML1  $\Delta$ Runt did not (supplemental Figure 3B). These data

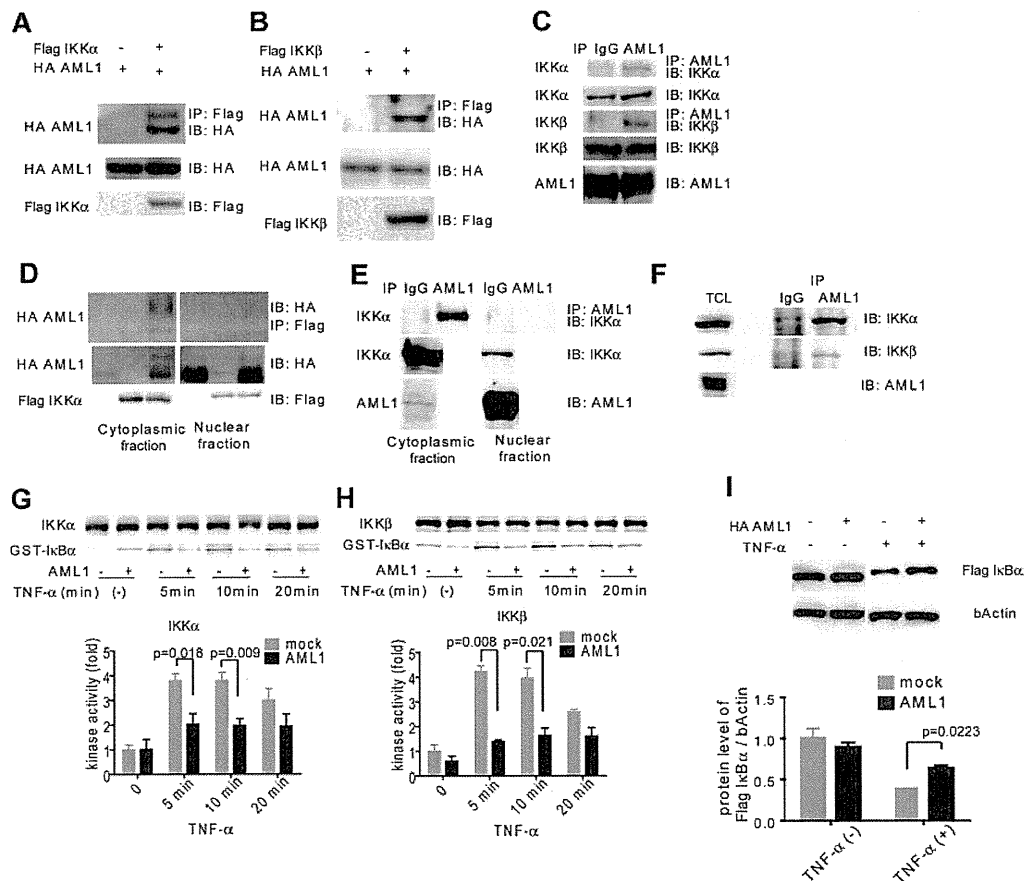


**Figure 4. AML1 physically interacts with IKK complex and inhibits its kinase activity.** (A-B) Interaction between AML1 and IKK complex. HEK293T cells were transfected with plasmids encoding for HA-AML1, FLAG-IKKα (A) and FLAG-IKKβ (B), as indicated, and extracts were immunoprecipitated with the antibody against FLAG. Western blots of the input lysate or immunoprecipitates were analyzed using the indicated antibodies. (C) Endogenous interaction between AML1 and the IKK complex in Jurkat cells. Cell extract from the Jurkat cells was immunoprecipitated with the antibody against AML1. Western blots of the input lysate or immunoprecipitates were analyzed using the indicated antibodies. (D) Interaction between AML1 and the IKK complex in cytoplasmic or nuclear fraction in HEK293T cells. (E) Endogenous interaction between AML1 and the IKK complex in cytoplasmic or nuclear fraction in Jurkat cells. (F) Endogenous interaction between AML1 and the IKK complex in U937 cells. Cell extract from the U937 cells was immunoprecipitated with the antibody against AML1. Western blots of the total lysate or immunoprecipitates were analyzed using the indicated antibodies. (G-H) In vitro kinase assays of IKKα (G) or IKKβ (H) in HEK293T cells transfected with AML1 or mock. Kinase activities were detected by autoradiography and quantified with ImageJ Version 1.41o software.<sup>31</sup> Error bars show mean  $\pm$  SEM. (I) Western blotting of IκBα degradation in HEK293T cells transfected with AML1 or mock. Protein levels of IκBα were quantified with ImageJ Version 1.41o software.<sup>31</sup> Error bars show mean  $\pm$  SEM.

indicate that C-terminal region with intact Runt domain of AML1 is required for inhibition of p53 nuclear translocation. We also assessed the physical interaction between each mutant of AML1 and IKK and found that all of the employed mutants retain the ability to interact with IKKα (supplemental Figure 3C). In addition, we found that D171N and S291fsX300 can interact with IKKα (supplemental Figure 2F). These results indicate that besides the physical interaction, there exists some additional mechanism that requires the integrity of AML1 for efficient inhibition of NF-κB by AML1.

#### AML1/ETO-positive leukemia is dependent on NF-κB signaling

Formation of chimeric genes because of chromosomal translocation is a major cause of AML1 dysfunction that leads to human leukemia. Among them, AML1/ETO, generated in t(8;21) leukemia, is one of the most frequent chimeric genes found in human leukemia. We examined how AML1/ETO affects NF-κB signaling. In contrast to AML1, AML1/ETO could not block nuclear translocation of p53 (Figure 6A). As is compatible with this observation, AML1/ETO has lost the ability to inhibit the kinase activity of IKKα and IKKβ, although it can physically

interacted with IKKα (Figure 6B-C and supplemental 4A). In addition, mouse bone marrow cells transformed by AML1/ETO showed enhanced nuclear localization of p53 compared with those immortalized by MLL/ENL (Figure 6D). In agreement with these findings, the growth of AML1/ETO-transformed cells was more susceptible to the NF-κB inhibitor BMS-345541, compared with MLL/ENL-transformed cells (Figure 6E-F). These results indicate a critical role of NF-κB signaling in hematopoietic cell transformation by AML1/ETO.

To evaluate activation of NF-κB signaling by AML1/ETO in human hematopoietic cells, we first used Kasumi-1 cells, a cell line derived from AML1/ETO-positive leukemia, and we examined their susceptibility to NF-κB inhibition. In Kasumi-1 cells, small amounts of AML1 and AML1/ETO were detected in the cytoplasmic fraction (supplemental Figure 4B). As shown in Figure 6G, proliferation of Kasumi-1 cells was more sensitive to BMS-345541 than that of THP-1 cells, a human leukemia cell line expressing MLL/AF9. Next, we analyzed in silico the previously reported gene expression data of human leukemias by Valk et al.<sup>28</sup> As shown in supplemental Figure 4C, NF-κB signaling was strongly activated in cluster 5, which was defined

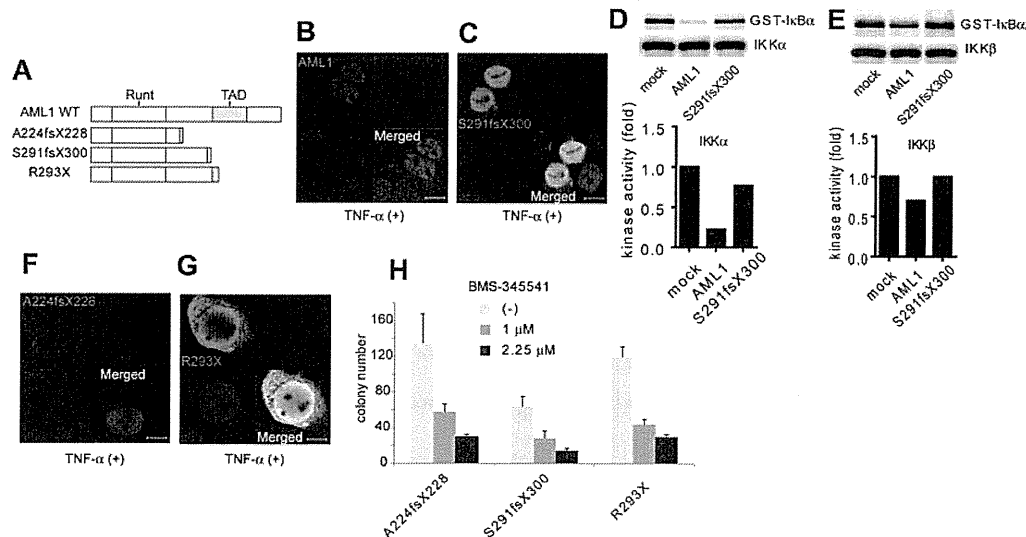


**Figure 5. A critical role of NF- $\kappa$ B signaling in the myeloid transformation induced by AML1 mutants.** (A) Schematic presentation of structures of the AML1 mutants. Runt indicates Runt domain, and TAD indicates transactivating domain. (B-C) Nuclear translocation assays of p65 in HEK293T cells transduced with AML1 mutants as indicated, 20 minutes after the addition of TNF- $\alpha$ . AML1 (B) and S291fsX300 (C). Scale bar represents 10  $\mu$ m. (D-E) In vitro kinase assays of IKK $\alpha$  (D) or IKK $\beta$  (E) in HEK293T cells transduced with AML1 or S291fsX300, 20 minutes after the addition of TNF- $\alpha$ . Kinase activities were detected by autoradiography and quantified with ImageJ Version 1.41o software.<sup>31</sup> (F-G) Nuclear translocation assays of p65 in HEK293T cells transduced with AML1 mutants as indicated, 20 minutes after the addition of TNF- $\alpha$ . A224fsX228 (F) and R293X (G). Scale bar represents 10  $\mu$ m. (H) Colony counts from the serial replating assays of AML1-mutants-transformed cells with BMS-345541. Error bars show mean  $\pm$  SEM.

by Valk et al according to gene expression profiles.<sup>28</sup> Remarkably, NF- $\kappa$ B signaling was activated in cluster 13, which contains patients with t(8;21), compared with any other clusters except cluster 5 (Figure 6H and supplemental Figure 4D). These results again indicate that NF- $\kappa$ B signaling is activated in AML1/ETO-positive leukemia and suggest that deregulated NF- $\kappa$ B signaling plays a significant role in AML1/ETO-induced transformation of hematopoietic cells.

#### Bortezomib ameliorates AML1-related leukemia in vivo

To assess the consequence of NF- $\kappa$ B inhibition on AML1-related leukemia in vivo, we used a mouse BMT model of AML1 S291fsX300.<sup>13</sup> We isolated spleen cells from leukemic mice that express AML1 S291fsX300 and transplanted them into sublethally irradiated (7.5 Gy) C57/B6 mice. These mice were treated with twice weekly injections of vehicle or bortezomib, a proteasome inhibitor that broadly inhibits NF- $\kappa$ B signaling (Figure 7A). As shown in Figure 7B, bortezomib significantly prolonged survival of the recipient mice compared with the vehicle-treated mice. Given that NF- $\kappa$ B signaling is not activated in MLL leukemia (Figure 6D-G), we used another leukemia mouse model generated by MLL/ENL as a control that is independent of NF- $\kappa$ B signaling. In contrast to the case with AML1 S291fsX300, bortezomib could not prolong survival of MLL/ENL leukemia mice (Figure 7C).

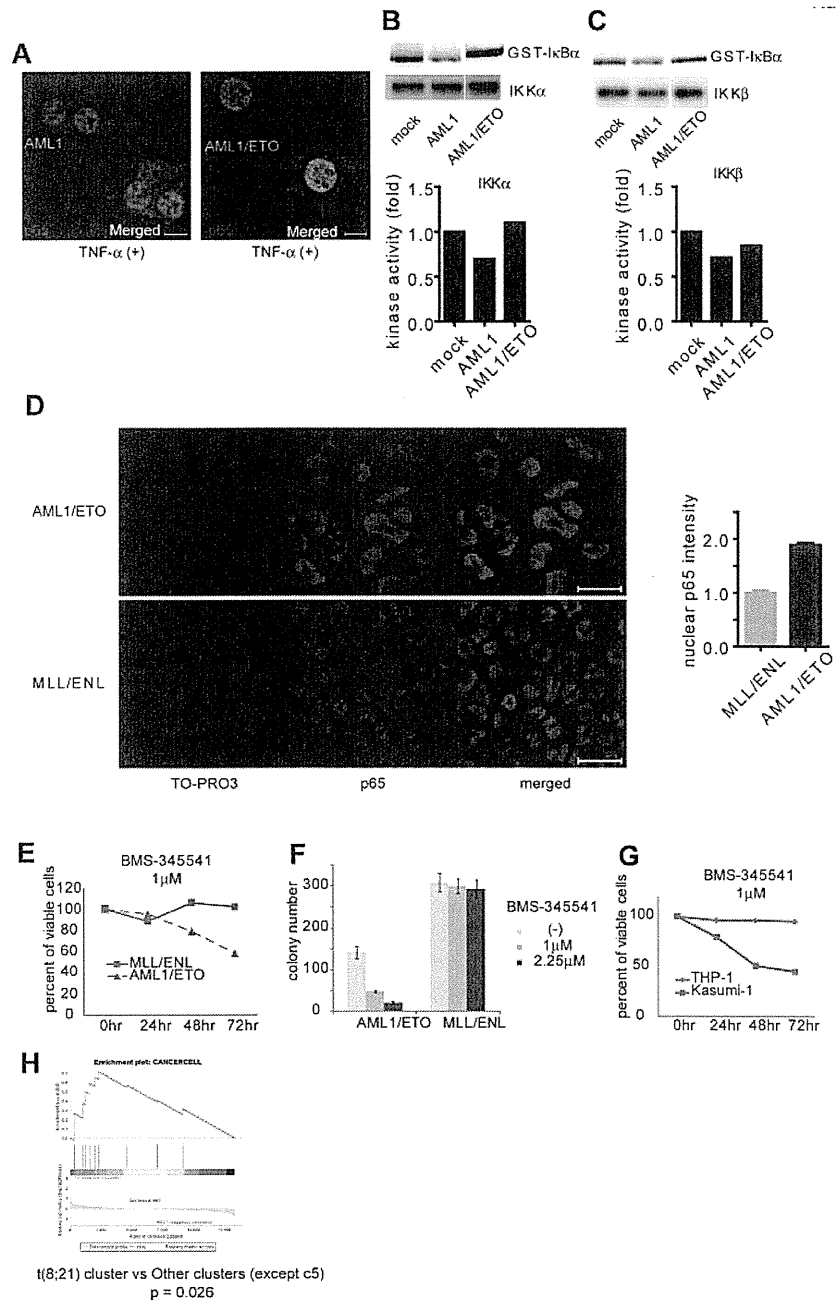
Next, we examined whether bortezomib can suppress AML1/ETO-induced leukemia in vivo. Because retroviral transduction of AML1/ETO alone cannot induce leukemia in mice,<sup>41</sup> we used an orthotopic cell line model of luciferase-positive SKNO-1 cells, a human AML cell line that expresses AML1/ETO (Figure 7D).<sup>33</sup> We transplanted SKNO-1 cells into sublethally irradiated NOG mice via tail vein and treated these mice with vehicle or bortezomib. Tumor burden was quantified using in vivo bioluminescence imaging. Mice were intraperitoneally injected with 150 mg/kg luciferin and imaged them with an IVIS imaging system 10 minutes after injection. Total body biolumi-

nescence was determined by in vivo bioluminescence imaging (IVIS Lumina2; Caliper Life Sciences) and quantitated using Living Image 2.60 software. In accordance with our results in vitro and in silico (Figure 6E-H), bortezomib significantly inhibited the growth of SKNO-1 cells in vivo (Figure 7E-F). Although bortezomib may have effects besides the NF- $\kappa$ B signaling inhibition, these results indicate that NF- $\kappa$ B signaling plays a critical role in the pathogenesis of myeloid tumors with deregulated AML1 function in vivo.

## Discussion

In this study, we found that targeted disruption, as well as leukemia-related gene alteration, of *AML1* results in the aberrant activation of NF- $\kappa$ B signaling. To detect immediate targets of AML1, we analyzed the gene expression profiles of LSK cells just after the synchronous inactivation of AML1 using the CreER system, and we captured the immediate alteration of target gene expression that is sometimes hidden by cell population shift or secondary changes in cellular signaling. Although changes in the expression of individual target genes were relatively subtle, we successfully identified NF- $\kappa$ B signaling to be a target subject to immediate regulation of AML1. The in vitro synchronous inactivation system may provide us with a useful tool that can find unidentified target signaling of transcription factors. Furthermore, by determining expression of several genes related to NF- $\kappa$ B signaling, we can select patients who are candidates for NF- $\kappa$ B-targeted therapy. This strategy should be effective especially when genetic mutations are unknown. Previously, Valk et al made unsupervised cluster analyses and identified 16 clusters of patients with AML on the basis of gene expression profiles.<sup>28</sup> We reanalyzed their gene expression data in silico and found that NF- $\kappa$ B signaling is highly activated in a cluster previously identified as "cluster 5." Valk et al found that cluster 5 was associated with poorer prognoses but that specific genetic changes have not been identified in this

**Figure 6. AML1/ETO-induced leukemic cells depend on NF- $\kappa$ B signaling.** (A) Nuclear translocation assays of p65 in HEK293T cells transduced with AML1 (left) or AML1/ETO (right), 20 minutes after the addition of TNF- $\alpha$ . Scale bar represents 10  $\mu$ m. (B-C) In vitro kinase assays of IKK $\alpha$  (B) or IKK $\beta$  (C) in HEK293T cells transduced with AML1 or AML1/ETO, 20 minutes after the addition of TNF- $\alpha$ . (D) Immunofluorescent staining of p65 in the BM cells transformed with AML1/ETO (top) or MLL/ENL (bottom). Scale bar represents 10  $\mu$ m. Blue indicates TO-PRO3 (nucleus), and red indicates p65. The mean intensity of nuclear localized p65 was quantified with ImageJ Version 1.41o software.<sup>31</sup> (E) Comparison of sensitivities between AML1/ETO-transformed cells with MLL/ENL-transformed cells in liquid culture. (F) Colony counts from the serial replating assay of AML1/ETO- or MLL/ENL-transformed cells with BMS-345541. Error bars show mean  $\pm$  SEM (G) Comparison of sensitivities between Kasumi-1 cells (AML1/ETO) with THP-1 cells (MLL/AF9) in liquid culture. (H) Enrichment of NF- $\kappa$ B target genes in t(8;21) leukemia cluster (c13) compared with other clusters (except c5).<sup>28</sup>



cluster.<sup>28</sup> In addition to t(8;21)-positive leukemia, the clinical activity of NF- $\kappa$ B inhibitors in AML cases belonging to this cluster warrants further investigation.

Although *AML1* mutations that lead to functional impairment have been frequently discovered in AML and MDS, it remains very difficult to develop a molecularly targeted therapy against deregulated *AML1* function, as is often the case with leukemia-related transcription factors. We discovered that NF- $\kappa$ B signaling is distinctly activated as a consequence of *AML1* mutation found in human leukemia. In the current study, bortezomib, a clinically available drug that can inhibit NF- $\kappa$ B signaling, has shown a significant activity against *AML1*-related leukemia. A wide variety of small molecules that inhibit NF- $\kappa$ B signaling are now being

developed and can become attractive candidates for targeted therapy of *AML1*-related leukemia in the future.

Although the amount of *AML1* in the cytoplasm is lower than that in the nucleus, we show that the physical interaction between *AML1* and IKK complex mainly occurs in the cytoplasm. In addition, the finding that *AML1* inhibits the nuclear translocation of p65 that is tightly regulated by the cytoplasmic IKK complex supports the cytoplasmic function of *AML1*. Although nuclear exporting signal was not reported in *AML1*, IKK may export *AML1* to the cytoplasmic fraction. We identified both *AML1* and *AML1/ETO* protein in the cytoplasmic fraction of Kasumi-1 cells in supplemental Figure 4B. The amounts of *AML1* and *AML1/ETO* protein in the cytoplasm are

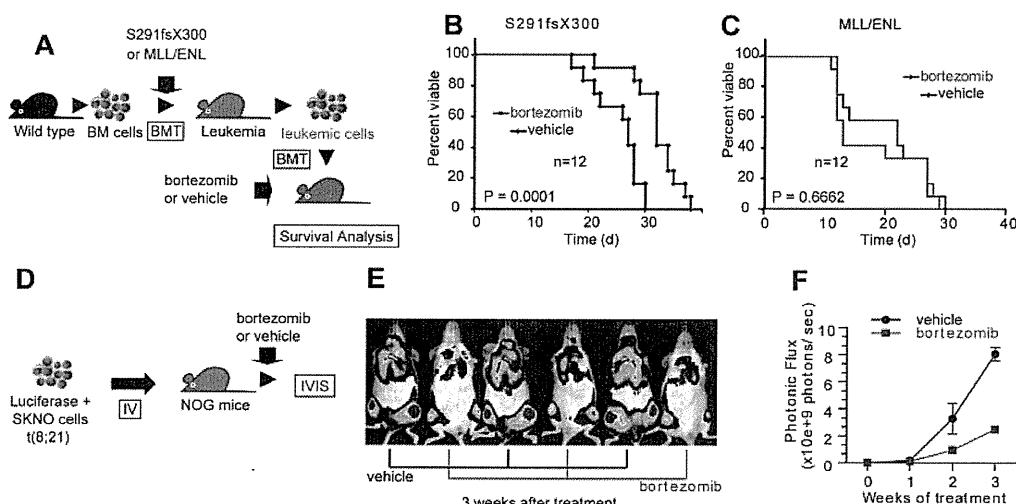


**Figure 7. Bortezomib inhibits the proliferation of leukemic cells with AML1 S291fsX300 or AML1/ETO in vivo.** (A) Schematic representation of the following experiments. Spleen cells isolated from S291fsX300-expressing leukemia mice were transplanted into sublethally irradiated (7.5 Gy) recipient mice. These mice were treated with twice weekly injections of vehicle or bortezomib. (B) Survival curves of mice transplanted with S291fsX300-induced leukemic cells treated with vehicle or bortezomib. Each group contains 12 mice. (C) Survival curves of mice transplanted with MLL/ENL-induced leukemic cells treated with vehicle or bortezomib. Each group contains 12 mice. The overall survival of mice in BM transplantation assays was analyzed by log-rank (Mantel-Cox) test. (D) Schematic representation of the following experiments. Luciferase positive SKNO-1 cells were injected into sublethally irradiated (2.0 Gy) NOG mice via tail vein, and these mice were treated with twice weekly injections of vehicle or bortezomib. (E-F) Tumor burden was quantified using in vivo bioluminescence imaging. Each group contains 3 mice.

fairly small. One possibility is that these proteins translocate between the cytoplasm and the nucleus in a context dependent manner. Another possibility is that AML1/ETO sequesters some components necessary for AML1 to inhibit IKK complex. A function of transcription factors that is exerted in the cytoplasm is well documented in p53.<sup>42</sup> Besides acting in the nucleus as a transcription factor to regulate expression of genes involved in apoptosis and cell cycle regulation, p53 triggers apoptosis and inhibits autophagy in the cytoplasm through a variety of processes, including induction of mitochondrial outer membrane permeabilization, direct regulation BAX activity, inhibition of AMP-dependent kinase, and activation of mammalian target of rapamycin. Revealing cytoplasmic functions of transcription factors will provide a new perspective for the therapy against malignancy with deregulated transcription factors.

Our data, however, do not deny the contribution of the transcriptional function of AML1 in inhibiting NF- $\kappa$ B signaling. It may be possible that AML1 attenuates NF- $\kappa$ B signaling transcriptionally and via the inducible IKK complex like Notch1.<sup>20</sup>

AML1 mutants including AML1/ETO tested in our study fail to inhibit kinase activity of IKKs, although they can physically interact with IKK complex. Therefore, it is likely that additional mechanism exists for wild-type AML1 to repress IKK activity after binding to IKK complex, which should be inactivated in AML1 mutants. One possible mechanism is that AML1 disturbs the formation of IKK complex. Another possibility is that AML1 blocks the interaction between IKK complex with upstream kinase or downstream substrates, such as I $\kappa$ B $\alpha$  or p65. Importantly, critical for the repression of IKK is C-terminal region, a region that may directly inhibit the IKK complex or to which some cofactor may bind. D171N cannot repress IKK activity, although it possesses the intact C-terminal region, and a conformational change caused by the point mutation may impair the inhibitory effect against IKK. Because AML1 mutants in this study can bind to IKK complex but do not attenuate IKK activity,

it is assumed that they exert a dominant-negative effect against wild-type AML1.

In normal hematopoiesis, AML1 suppresses NF- $\kappa$ B signaling and thus may contribute to inhibition of excessive proliferation of hematopoietic cells. Aberrant activation of NF- $\kappa$ B signaling may cause expansion of HSCs in AML1 cKO mice. Although it is reported that neither p65 nor a constitutively active form of IKK increases the number of human cord blood cells when transduced in vitro, intact AML1 may inhibit the NF- $\kappa$ B signaling in these cells.<sup>43</sup> It also is reported that NF- $\kappa$ B signaling is more activated in leukemic stem cells than normal HSCs.<sup>44</sup> In leukemic cells, the NF- $\kappa$ B inhibitory mechanism including AML1 may be disrupted. Once genetic mutation of AML1 occurs in hematopoietic cells, aberrant activation of NF- $\kappa$ B signaling exerts antiapoptotic and proliferation-promoting effects via activation of BCL-XL or JUNB. Proliferative advantage conferred by activated NF- $\kappa$ B signaling may contribute to the clonal evolution of AML1-mutated cells that leads to leukemic transformation. Conversely, it is known that activation of NF- $\kappa$ B signaling causes myeloproliferative disease via the stroma-mediated signaling.<sup>45</sup> Thus, germ line mutation of AML1 that occurs in familial platelet disorder patients may contribute to leukemogenesis in those patients not only via a hematopoietic cell-autonomous function but also via niche-derived signaling.<sup>7</sup>

Both of AML1 and NF- $\kappa$ B play important roles in lymphocyte differentiation.<sup>11,46</sup> Well documented is the pathogenetic significance of NF- $\kappa$ B signaling in autoimmune diseases, especially rheumatoid arthritis (RA).<sup>47</sup> Disease-associated single-nucleotide polymorphisms in autoimmune diseases are found in AML1 binding sites of several gene promoters: SLC9A3R1 and NAT9 in psoriasis; SLC22A4 in RA; and PDCD1 in systemic lupus erythematosus.<sup>48-50</sup> A single-nucleotide polymorphism in AML1 per se also is associated with RA.<sup>49</sup> Along with this study, AML1 may contribute to the pathogenesis of autoimmune diseases through the cytoplasmic function to modulate NF- $\kappa$ B activity as well as the nuclear function as a transcription factor.

In summary, our experiments identified direct regulation of NF- $\kappa$ B signaling by AML1. AML1 negatively regulates NF- $\kappa$ B signaling by inhibiting kinase activity of IKK. Furthermore, mutated forms of AML1 found in MDS or AML fail to inhibit NF- $\kappa$ B signaling. NF- $\kappa$ B signaling can be a promising molecular target for the treatment of AML1-related hematologic malignancies.

materials and instruments; and M. Kobayashi, S. Naito, Y. Sawamoto, and Y. Shimamura for expert technical assistance.

This study was supported in part by grants from the Ministry of Education, Culture, Sports, Science and Technology (Japan).

## Acknowledgments

The authors thank Drs D. E. Zhang (University of California—San Diego), T. D. Gilmore (Boston University), S. W. Hiebert (Vanderbilt University), H. Nakauchi (Institute of Medical Science [IMS], University of Tokyo), T. Kitamura (IMS, University of Tokyo), H. Harada (University of Hiroshima), S. Ogawa (University of Tokyo), T. Nosaka (University of Mie), P. Chambon (Institut de Génétique et Biologie Moléculaire et Cellulaire), and Andrew L. Kung (Dana-Farber Cancer Institute); Kyowa Hakko Kirin Co Ltd; and Wakunaga Pharmaceutical Co Ltd for providing essential

## Authorship

Contribution: M.N. conceived of and designed the research, performed experiments and analyses, and wrote the paper; M.S., N.W.-O., S.A., A.Y., A.S., N.N., K. Kataoka, and T.S. performed experiments; M.I., K. Kumano, Y.N., and Y.I. wrote the paper; and M.K. supervised the whole project and wrote the paper.

Conflict-of-interest disclosure: The authors declare no competing financial interests.

Correspondence: Mineo Kurokawa, Department of Hematology and Oncology, Graduate School of Medicine, University of Tokyo, 7-3-1 Hongo, Bunkyo-ku, Tokyo 113-8655, Japan; e-mail: kurokawa-ky@umin.ac.jp.

## References

- Selivanova G, Wiman KG. Reactivation of mutant p53: molecular mechanisms and therapeutic potential. *Oncogene*. 2007;26(15):2243-2254.
- Miyoshi H, Shimizu K, Kozu T, Maseki N, Kaneko Y, Ohki M. t(8;21) breakpoints on chromosome 21 in acute myeloid leukemia are clustered within a limited region of a single gene, AML1. *Proc Natl Acad Sci U S A*. 1991;88(23):10431-10434.
- Harada H, Harada Y, Niimi H, Kyo T, Kimura A, Inaba T. High incidence of somatic mutations in the AML1/RUNX1 gene in myelodysplastic syndrome and low blast percentage myeloid leukemia with myelodysplasia. *Blood*. 2004;103(6):2316-2324.
- Imai Y, Kurokawa M, Izutsu K, et al. Mutations of the AML1 gene in myelodysplastic syndrome and their functional implications in leukemogenesis. *Blood*. 2000;96(9):3154-3160.
- Tang JL, Hou HA, Chen CY, et al. AML1/RUNX1 mutations in 470 adult patients with de novo acute myeloid leukemia: prognostic implication and interaction with other gene alterations. *Blood*. 2009;114(26):5352-5361.
- Schnittger S, Dicker F, Kern W, et al. RUNX1 mutations are frequent in de novo AML with noncomplex karyotype and confer an unfavorable prognosis. *Blood*. 2011;117(8):2348-2357.
- Song WJ, Sullivan M, Legare RD, et al. Haploinsufficiency of CBFA2 causes familial thrombocytopenia with propensity to develop acute myelogenous leukaemia. *Nat Genet*. 1999;23(2):166-175.
- Okuda T, van Deursen J, Hiebert SW, Grosveld G, Downing JR. AML1, the target of multiple chromosomal translocations in human leukemia, is essential for normal fetal liver hematopoiesis. *Cell*. 1996;84(2):321-330.
- Wang Q, Stacy T, Binder M, Marin-Padilla M, Sharpe AH, Speck NA. Disruption of the Cbfa2 gene causes necrosis and hemorrhaging in the central nervous system and blocks definitive hematopoiesis. *Proc Natl Acad Sci U S A*. 1996;93(8):3444-3449.
- Ichikawa M, Goyama S, Asai T, et al. AML1/RUNX1 negatively regulates quiescent hematopoietic stem cells in adult hematopoiesis. *J Immunol*. 2008;180(7):4402-4408.
- Ichikawa M, Asai T, Saito T, et al. AML-1 is required for megakaryocytic maturation and lymphocytic differentiation, but not for maintenance of hematopoietic stem cells in adult hematopoiesis. *Nat Med*. 2004;10(3):299-304.
- Harada H, Harada Y, Tanaka H, Kimura A, Inaba T. Implications of somatic mutations in the AML1 gene in radiation-associated and therapy-related myelodysplastic syndrome/acute myeloid leukemia. *Blood*. 2003;101(2):673-680.
- Watanabe-Okochi N, Kitaura J, Ono R, et al. AML1 mutations induced MDS and MDS/AML in a mouse BMT model. *Blood*. 2008;111(8):4297-4308.
- Huang G, Zhang P, Hirai H, et al. PU. 1 is a major downstream target of AML1 (RUNX1) in adult mouse hematopoiesis. *Nat Genet*. 2008;40(1):51-60.
- de Bruijn MF, Speck NA. Core-binding factors in hematopoiesis and immune function. *Oncogene*. 2004;23(24):4238-4248.
- Hayden MS, Ghosh S. Shared principles in NF-kappaB signaling. *Cell*. 2008;132(3):344-362.
- Dejardin E. The alternative NF-kappaB pathway from biochemistry to biology: pitfalls and promises for future drug development. *Biochem Pharmacol*. 2006;72(9):1161-1179.
- Lombardi L, Ciana P, Cappellini C, et al. Structural and functional characterization of the promoter regions of the NFKB2 gene. *Nucleic Acids Res*. 1995;23(12):2328-2336.
- Karin M. Nuclear factor-kappaB in cancer development and progression. *Nature*. 2006;441(7092):431-436.
- Vilimas T, Mascarenhas J, Palomero T, et al. Targeting the NF-kappaB signaling pathway in Notch1-induced T-cell leukemia. *Nat Med*. 2007;13(1):70-77.
- Annunziata CM, Davis RE, Demchenko Y, et al. Frequent engagement of the classical and alternative NF-kappaB pathways by diverse genetic abnormalities in multiple myeloma. *Cancer Cell*. 2007;12(2):115-130.
- Keats JJ, Fonseca R, Chesi M, et al. Promiscuous mutations activate the noncanonical NF-kappaB pathway in multiple myeloma. *Cancer Cell*. 2007;12(2):131-144.
- Morita S, Kojima T, Kitamura T. Plat-E: an efficient and stable system for transient packaging of retroviruses. *Gene Ther*. 2000;7(12):1063-1066.
- Nakagawa M, Ichikawa M, Kumano K, et al. AML1/RUNX1 rescues Notch1-null mutation-induced deficiency of para-aortic splanchnopleural hematopoiesis. *Blood*. 2006;108(10):3329-3334.
- Goyama S, Yamamoto G, Shimabe M, et al. Evi-1 is a critical regulator for hematopoietic stem cells and transformed leukemic cells. *Cell Stem Cell*. 2008;3(2):207-220.
- Li C, Hung Wong W. Model-based analysis of oligonucleotide arrays: model validation, design issues and standard error application. *Genome Biol*. 2001;2(8):RESEARCH0032.
- Subramanian A, Tamayo P, Mootha VK, et al. Gene set enrichment analysis: a knowledge-based approach for interpreting genome-wide expression profiles. *Proc Natl Acad Sci U S A*. 2005;102(43):15545-15550.
- Valk PJ, Verhaak RG, Beijnen MA, et al. Prognostically useful gene-expression profiles in acute myeloid leukemia. *N Engl J Med*. 2004;350(16):1617-1628.
- Krejci O, Wunderlich M, Geiger H, et al. p53 signaling in response to increased DNA damage sensitizes AML1-ETO cells to stress-induced death. *Blood*. 2008;111(4):2190-2199.
- Wei J, Wunderlich M, Fox C, et al. Microenvironment determines lineage fate in a human model of MLL-AF9 leukemia. *Cancer Cell*. 2008;13(6):483-495.
- Abramoff MD, Magelhaes PJ, Ram SJ. Image processing with ImageJ. *Biophotonics Int*. 2004;11(7):36-42.
- Lagna G, Hata A, Hemmati-Brivanlou A, Massague J. Partnership between DPC4 and SMAD proteins in TGF-beta signalling pathways. *Nature*. 1996;383(6603):832-836.
- Corsello SM, Roti G, Ross KN, et al. Identification of AML1-ETO modulators by chemical genomics. *Blood*. 2009;113(24):6193-6205.
- Park KJ, Choi SH, Lee SY, Hwang SB, Lai MM. Nonstructural 5A protein of hepatitis C virus modulates tumor necrosis factor alpha-stimulated nuclear factor kappa B activation. *J Biol Chem*. 2002;277(15):13122-13128.
- Indra AK, Warot X, Brocard J, et al. Temporally-controlled site-specific mutagenesis in the basal layer of the epidermis: comparison of the recombinase activity of the tamoxifen-inducible Cre-ER(T) and Cre-ER(T2) recombinases. *Nucleic Acids Res*. 1999;27(22):4324-4327.
- Mootha VK, Lindgren CM, Eriksson KF, et al.

- PGC-1 $\alpha$ -responsive genes involved in oxidative phosphorylation are coordinately downregulated in human diabetes. *Nat Genet.* 2003;34(3):267-273.
37. Hinata K, Gervin AM, Jennifer Zhang Y, Khavari PA. Divergent gene regulation and growth effects by NF- $\kappa$ B in epithelial and mesenchymal cells of human skin. *Oncogene.* 2003;22(13):1955-1964.
  38. Tian B, Nowak DE, Jamaluddin M, Wang S, Brasier AR. Identification of direct genomic targets downstream of the nuclear factor- $\kappa$ B transcription factor mediating tumor necrosis factor signaling. *J Biol Chem.* 2005;280(17):17435-17448.
  39. Hanson JL, Hawke NA, Kashatus D, Baldwin AS. The nuclear factor  $\kappa$ B subunits RelA/p65 and c-Rel potentiate but are not required for Ras-induced cellular transformation. *Cancer Res.* 2004;64(20):7248-7255.
  40. Kuo MC, Liang DC, Huang CF, et al. RUNX1 mutations are frequent in chronic myelomonocytic leukemia and mutations at the C-terminal region might predict acute myeloid leukemia transformation. *Leukemia.* 2009;23(8):1426-1431.
  41. Yan M, Kanbe E, Peterson LF, et al. A previously unidentified alternatively spliced isoform of t(8;21) transcript promotes leukemogenesis. *Nat Med.* 2006;12(8):945-949.
  42. Green DR, Kroemer G. Cytoplasmic functions of the tumour suppressor p53. *Nature.* 2009;458(7242):1127-1130.
  43. Schepers H, Eggen BJ, Schuringa JJ, Vellenga E. Constitutive activation of NF- $\kappa$ B is not sufficient to disturb normal steady-state hematopoiesis. *Haematologica.* 2006;91(12):1710-1711.
  44. Guzman ML, Swiderski CF, Howard DS, et al. Preferential induction of apoptosis for primary human leukemic stem cells. *Proc Natl Acad Sci U S A.* 2002;99(25):16220-16225.
  45. Rupec RA, Jundt F, Rebholz B, et al. Stroma-mediated dysregulation of myelopoiesis in mice lacking I  $\kappa$ B  $\alpha$ . *Immunity.* 2005;22(4):479-491.
  46. Bottero V, Withoff S, Verma IM. NF- $\kappa$ B and the regulation of hematopoiesis. *Cell Death Differ.* 2006;13(5):785-797.
  47. Criswell LA. Gene discovery in rheumatoid arthritis highlights the CD40/NF- $\kappa$ B signaling pathway in disease pathogenesis. *Immunol Rev.* 2010;233(1):55-61.
  48. Prokunina L, Castillejo-Lopez C, Oberg F, et al. A regulatory polymorphism in PDCD1 is associated with susceptibility to systemic lupus erythematosus in humans. *Nat Genet.* 2002;32(4):666-669.
  49. Tokunishi S, Yamada R, Chang X, et al. An intronic SNP in a RUNX1 binding site of SLC22A4, encoding an organic cation transporter, is associated with rheumatoid arthritis. *Nat Genet.* 2003;35(4):341-348.
  50. Helms C, Cao L, Krueger JG, et al. A putative RUNX1 binding site variant between SLC9A3R1 and NAT9 is associated with susceptibility to psoriasis. *Nat Genet.* 2003;35(4):349-356.



## Loss of AML1/Runx1 accelerates the development of MLL-ENL leukemia through down-regulation of p19<sup>ARF</sup>

\*Nahoko Nishimoto,<sup>1</sup> \*Shunya Arai,<sup>1</sup> Motoshi Ichikawa,<sup>1</sup> Masahiro Nakagawa,<sup>1</sup> Susumu Goyama,<sup>1</sup> Keiki Kumano,<sup>1</sup> Tsuyoshi Takahashi,<sup>1</sup> Yasuhiko Kamikubo,<sup>1</sup> Yoichi Imai,<sup>1</sup> and Mineo Kurokawa<sup>1</sup>

<sup>1</sup>Department of Hematology and Oncology, Graduate School of Medicine, University of Tokyo, Tokyo, Japan

**Dysfunction of AML1/Runx1, a transcription factor, plays a crucial role in the development of many types of leukemia. Additional events are often required for AML1 dysfunction to induce full-blown leukemia; however, a mechanistic basis of their cooperation is still elusive. Here, we investigated the effect of AML1 deficiency on the development of MLL-ENL leukemia in mice. *Aml1* excised bone**

**marrow cells lead to MLL-ENL leukemia with shorter duration than *Aml1* intact cells in vivo. Although the number of MLL-ENL leukemia-initiating cells is not affected by loss of AML1, the proliferation of leukemic cells is enhanced in *Aml1*-excised MLL-ENL leukemic mice. We found that the enhanced proliferation is the result of repression of p19<sup>ARF</sup> that is directly regulated by AML1 in MLL-ENL**

**leukemic cells. We also found that down-regulation of p19<sup>ARF</sup> induces the accelerated onset of MLL-ENL leukemia, suggesting that p19<sup>ARF</sup> is a major target of AML1 in MLL-ENL leukemia. These results provide a new insight into a role for AML1 in the progression of leukemia. (*Blood*. 2011; 118(9):2541-2550)**

### Introduction

AML1, also called RUNX1, CBFA2, or PEBP2 $\alpha$ B, was found at the breakpoint on chromosome 21 from acute myeloid leukemia (AML) patients with t(8;21)(q22;q22).<sup>1</sup> AML1 is a transcription factor that belongs to RUNX family proteins. It heterodimerizes with CBF $\beta$  and binds to the specific DNA sequence (TGT/CGGT), called the PEBP2 binding site.<sup>2-4</sup> AML1 regulates transcription of various genes related to normal hematopoiesis, and targeted disruption of AML1 in mice revealed that it is essential for definitive hematopoiesis during embryogenesis.<sup>5</sup> Conventional knockout mice are embryonic lethal because of hemorrhage in the central nervous system. We generated conditional knockout mice of AML1 to study a role of AML1 in adult hematopoiesis after birth.<sup>6</sup> These mice showed thrombocytopenia because of maturation block of megakaryocytes, perturbed lymphocyte development, and increase in the number of hematopoietic stem/progenitor cells.

The disruption of AML1 functions is highly related to occurrence of myeloid malignancies through chromosomal translocation or point mutation.<sup>7-9</sup> Although introduction of AML1-ETO, the fusion protein generated in AML with t(8;21) chromosomal translocation, into mouse bone marrow (BM) cells leads to proliferation of myeloid cells, it is not sufficient to induce leukemia without providing alkylating agents for the mice.<sup>10-14</sup> AML1-ETO acts as a dominant negative effector for wild-type AML1, and it is supposed that function of AML1 is lost in AML1-ETO-expressing cells. These results suggest that the other genetic change in addition to the loss of AML1 function is necessary for the development of full-blown leukemia. In mice, *c-Kit* and *FLT3-ITD* mutations are reported to collaborate with gene alteration of AML1 in leukemogenesis.<sup>15,16</sup> Furthermore, positive correlation between *c-Kit* mutations and AML1-ETO is reported in human cases.<sup>17,18</sup> However, precise molecular mechanisms that underlie the development of AML1-related leukemia are still to be elucidated.

We previously demonstrated that hematopoietic stem/progenitor cells are expanded in *Aml1*-deficient mice.<sup>19</sup> Expansion of the hematopoietic stem/progenitor cells is also observed in the mouse models of AML with t(8;21), in which the chimeric protein AML1-ETO suppresses the normal function of AML1. Expansion of the hematopoietic stem/progenitor cells is supposed to predispose the animals to full-blown leukemia when additional mutations occur in the proliferating cells.

Mixed lineage leukemia (MLL) is located on band q23 of the chromosome 11 and is frequently translocated in human leukemias. In addition to formation of fusion genes with > 50 partners, partial tandem duplication of MLL (MLL-PTD) is also found in human leukemias. Interestingly, in human leukemias without 11q23 chromosomal translocation, point mutations of *AML1* and *MLL-PTD* are frequently observed in the same patients.<sup>17</sup> This prompted us to speculate that AML1 loss and *MLL* mutations may cooperate in the development of human leukemia. To test this, we evaluated the effect of AML1 loss on MLL-related leukemia using a mouse model and found that loss of AML1 significantly accelerated the development of MLL-leukemia. We also found that p19<sup>ARF</sup>, a known target of AML1 and AML1-ETO,<sup>20</sup> plays a critical role in the leukemia acceleration caused by AML1 loss. These findings provide a novel mechanistic basis of cooperation between impaired AML1 function and other leukemia-related gene alteration.

### Methods

#### Mouse strains

*Aml1*<sup>flox/flox</sup> Mx-Cre (+) mice and *Aml1*<sup>flox/flox</sup> Mx-Cre (-) mice were previously described.<sup>6</sup> To induce *Aml1* deletion in vivo, mice were

Submitted October 24, 2010; accepted June 26, 2011. Prepublished online as *Blood* First Edition paper, July 14, 2011; DOI 10.1182/blood-2010-10-315440.

\*N.N. and S.A. contributed equally to this study.

The publication costs of this article were defrayed in part by page charge payment. Therefore, and solely to indicate this fact, this article is hereby marked "advertisement" in accordance with 18 USC section 1734.

© 2011 by The American Society of Hematology

intraperitoneally injected with 250  $\mu$ g of polyinosinic-polycytidylic acid (pIpC; Sigma-Aldrich) 3 times every other day and were used for the experiments after 4 to 8 weeks.<sup>6</sup> The genotypes of the loxP-flanked *Aml1* (*Aml1<sup>f</sup>*) and excised *Aml1* (*Aml1<sup>Δ</sup>*) loci were analyzed, using primers as described previously.<sup>6</sup> Eight- to 10-week-old female C57BL/6J mice were used as recipients in transplantation. Mice were kept at the Center for Disease Biology and Integrative Medicine, University of Tokyo, according to institutional guidelines. All animal experiments were approved by the University of Tokyo Institutional Animal Care and Use Committee.

### Retrovirus infection

The cDNA of MLL-ENL (generous gift from Toshio Kitamura) was subcloned into the *EcoRI* site of pMSCV-neo (Clontech).<sup>21</sup> To produce MLL-ENL-expressing retrovirus, Plat-E packaging cells (generous gift from Toshio Kitamura) or Ecopack2-293 cells (Clontech) were transiently transfected with retroviral constructs, as described previously.<sup>22,23</sup> To produce green fluorescent protein (GFP)- or AML1-GFP-expressing retrovirus, we used cMP34 packaging cells.<sup>24</sup> Two retrovirus vectors expressing small hairpin RNAs were constructed for p19<sup>ARF</sup>.<sup>25</sup> After transfection, puromycin-resistant cells were selected in medium (RPMI with 20% FCS, 10 ng/mL IL-3) containing 2  $\mu$ g/mL puromycin for 3 days.

### Colony replating assay

The cells infected with retrovirus were washed by PBS and resuspended in IMDM (with 2% FCS), and  $1 \times 10^5$  cells were plated in the 35-mm plate with Methocult M3434 (StemCell Technologies) containing 10 ng/mL of murine GM-CSF and 0.8 mg/mL of G418. After 7 days, the cells were collected and washed by PBS twice. A total of  $1 \times 10^4$  cells were plated in the same semisolid culture medium without G418. Colony counting and replating were performed every 7 days.

### Transplantation assay

A total of  $1 \times 10^6$  of cells infected with retrovirus were injected into sublethally irradiated (x-ray, 7.5 Gy) recipient mice via the tail vein. To transplant leukemic cells into recipient mice, mononuclear cells isolated from the spleen of leukemic mice were infected with retrovirus and injected into sublethally irradiated (7.5 Gy) recipient mice via the tail vein.

### In vitro liquid culture

Leukemic or immortalized cells were cultured in RPMI medium containing 20% FCS and 10 ng/mL of IL-3. In apoptotic cell analyses, liquid culture medium without IL-3 was also used.

### Quantitative real-time PCR

Quantitative real-time PCR was performed as described previously.<sup>26</sup> mRNA expression levels of all genes, relative to those of normal BM mononuclear cells, were normalized to *Gapdh*. The primers used are as follows: *Aml1*: TaqMan Gene Expression Assay (Applied Biosystems; Assay ID Mm00486762\_m1); *Gapdh*: forward, TGGTGAAGCAG-GCATCTGAG; reverse, TGCTGTTGAAGTCGCAGGAG; *p19<sup>ARF</sup>*: forward, CATGTTGTTGAGGCTAGAGAGG; reverse, TCGAATCTGCAC-CGTAGTTG; *p21<sup>CIP1</sup>*: forward, CTGTTCCGCACAGGAGCAA; reverse, ACGGCACAATGCTACT/TaqMan probe TGTGCCGTTGTCTCT-TCGGTCCC (Applied Biosystems); *p53*: forward, CACAGCGTGGTG-GTACCTTATG; reverse, TTCCAGTGTGATGATGGTAAGGA/TaqMan probe CCACCCGAGGCCGGCTCTG (Applied Biosystems); *p27<sup>KIP1</sup>*: forward, GGCCCGTCAATCATGAA; reverse, TTGCGCT-GACTCGCTTCTC; *p15<sup>INK4B</sup>*: forward, TCAGAGACCAGGCTGTAG-CAA; reverse, CCCCCTGCTG; *Bax*: forward, AAAATGGCCAGTGAA-GAGCA; reverse, GTGAGCGGCTGCTGTCT/TaqMan probe (Roche

Universal Probe Library #83); *p16<sup>INK4A</sup>*: forward, CCCAACGC-CCCGAACT; reverse, GTGAACGTTGCCCATCATCA; *PU.1*: forward, GGAGAAGCTGATGGCTTGG; reverse, CAGGCGAATCTTT-TTCTTGC TaqMan probe (Roche Universal Probe Library #94); *Bmi1*: forward, AAACCAGACCACTCCTGAACA; reverse, TCTTCTTC-TCTTCATCTCATTTTTGA/TaqMan probe (Roche Universal Probe Library #20); *Hoxa5*: forward, GCAAGCTGCACATTAGTCAC; reverse, GCATGAGCTATTTCGATCCT; *Hoxa7*: forward, CTCTTTCTTC-CACCTCATGCGCCGA; reverse, TGCGCCTCCTACGACCAAAA-CATC; *Hoxa9*: forward, TCCCTGACTGACTATGCTTGTG; reverse, GTTGGCAGCCGGTTATT/TaqMan probe (Roche Universal Probe Library #25); *Hoxa10*: forward, GGAAGGAGCGAGTCCTAGA; reverse, TTCATTGTCTGTCCGTGAG; *Meis1*: forward, TTGTAATG-GACGGTCAGCAG; reverse, GCTACATACTCCCTGGCATA/Taq-Man probe (Roche Universal Probe Library #105); *Gapdh* promoter: forward, CACAAACAGGACCCAACATT; reverse, ATGAAGTGTC-CCTCCTTGTG; *p19<sup>ARF</sup>* AML1 binding site (distal): forward, AGTTA-ACCGGAGCGAAAGCC; reverse, CACCCATCGCGGTGACAG; *p19<sup>ARF</sup>* AML1 binding site (proximal): forward, GGATTACAACCTA-CACCTGCGGTC; reverse, CCACAGATTCTATTTTTACGCAC.

### Flow cytometric analysis

Cells were sorted with FACSAria, and analysis was performed on an LSRII (BD Biosciences). To analyze the cell surface antigen, anti-Mac-1 (phycoerythrin-conjugated), Gr-1 (allophycocyanin), CD117 (allophycocyanin), and Sca-1 (phycoerythrin; BD Biosciences) were used. To analyze the cell-cycle status, cells were stained with propidium iodide (BD Biosciences) at room temperature for 30 minutes. Apoptosis was assayed by annexin V and propidium iodide staining. To analyze the intracellular protein levels, cells were fixed and permeabilized with fixation/permeabilization solution (BD Cytofix/Cytoperm Fixation/Permeabilization kit) following the manufacturer's protocol, before incubation with antibodies. Fixed cells were incubated with either anti-p53 (1C12) mouse monoclonal antibody (AlexaFluor-647-conjugated) or mouse (MOPC-21) monoclonal antibody IgG1 isotype control (AlexaFluor-647-conjugated; Cell Signaling Technology) at room temperature for 60 minutes. The geometric mean fluorescence intensity was calculated by the subtraction of that of the cells stained with isotype control IgG1 from that of the cells stained with anti-p53 antibodies.

### ChIP assay

ChIP assays were performed as described earlier,<sup>27</sup> with minor modifications. A total of  $1 \times 10^7$  of splenocytes from leukemic mice were crosslinked with 1% formaldehyde. Subsequently, chromatin was fragmented by sonication to obtain an average fragment length of 200-900 bp (Bronson Sonifier 250). After the chromatin fraction was incubated with normal rabbit IgG (Abcam) or polyclonal rabbit AML1/Runx1 antibody (Active Motif), immune complexes were bound to Dynabeads protein G (Invitrogen). Eluted DNA samples were then analyzed by quantitative real-time PCR using specific primer pairs listed in the primers for quantitative real-time PCR. PCR results were calculated validly using the  $\Delta\Delta C_t$  method.

### Luciferase reporter assay

The mouse *p19<sup>ARF</sup>* promoter region was obtained by PCR with the following primers: forward, GCCGTACCGTACCGCTAAGGGTCAAAAACGCC; reverse, GCGAGATCTCTACAGTGACCAAGAACCCTGCGAC. This fragment was subcloned into luciferase reporter vector, pGL4.10. Mutations of the PEBP2 sites in the *p19<sup>ARF</sup>* promoter construct were introduced by QuickChange site-directed mutagenesis kit (Stratagene) using the following primers: forward, CCGCGGCGTGGCTGTCAAAAAAATGGGTGGCGAGCGAAGC; reverse, GCTTCGCTCGCCACCCATTTTTTTGACAGCCAGCGCCGCGG. For reporter assays, COS-7 cells were seeded in 12-well culture plates at a density of  $1 \times 10^5$  cells per well. At 6 hours after seeding, the cells were transfected with 200 ng of each luciferase reporter construct, together with 200 ng of each appropriate expression plasmid (eg, pME18S vector [Mock], pME18S-AML1)

using FuGENE 6 (Roche Diagnostics). The cells were harvested 40 hours after transfection, and luciferase activities were analyzed. CMV  $\beta$ -gal expression vector was also cotransfected for normalization of transfection efficiency. Results are expressed as fold activation with SD.

### Statistical analysis

To compare data between groups, unpaired Student *t* test was used when equal variance was met by the F test. When unequal variances were detected, the Welch *t* test was used. Differences were considered statistically significant at a *P* value < .05. Statistical analyses were performed using the statistical software package R Version 2.13.0.

## Results

### Proliferation of MLL-ENL–transduced hematopoietic precursors is enhanced on AML1 deletion

To examine the effect of AML1 deletion on proliferation of MLL leukemic cells, we retrovirally transduced BM progenitors from *Aml1*<sup>flox/flox</sup>; Mx-Cre(–; *Aml1*<sup>fl/fl</sup>) or *Aml1*<sup>flox/flox</sup>; Mx-Cre(+) mice that had been injected with pIpC (*Aml1* <sup>$\Delta/\Delta$</sup> ), with MLL-ENL vector (Figure 1A). As shown in the previous study, MLL-ENL-infected BM progenitors were immortalized and proliferated in the methylcellulose culture.<sup>21</sup> Cre-mediated recombination was confirmed by genomic PCR in the BM cells harvested from the pIpC-treated *Aml1*<sup>flox/flox</sup>; Mx-Cre(+) mice (Figure 1B). The absence of AML1 mRNA was additionally confirmed by quantitative reverse-transcribed PCR of *Aml1*-excised immortalized cells (Figure 1C). We transferred these immortalized cells into liquid cultures in the presence of IL-3. Although growth of the cells differed immediately after the initiation of liquid cultures, each type of cells showed exponential growth after several days (Figure 1D-E). After day 9, *Aml1*-excised immortalized cells proliferated significantly faster than the *Aml1* intact controls (*P* < .001, Figure 1E). These results indicate that the proliferation of MLL-ENL-transformed cells is enhanced in the absence of AML1. *Aml1*-excised transformed cells were Gr-1<sup>+</sup>, Mac-1<sup>+</sup>, Sca1<sup>–</sup>, and c-Kit<sup>low</sup>–, which was not significantly different from control cells (Figure 1F). Morphologic changes were neither observed (data not shown).

### Loss of AML1 accelerates leukemia onset in MLL-ENL mice

Our in vitro studies showed that loss of AML1 enhances the proliferation of MLL-ENL–transformed cells. These results suggest that loss of AML1 accelerates the onset of MLL-ENL leukemia. To test this, we retrovirally transduced MLL-ENL into *Aml1*-intact or -excised BM progenitors. Those cells were transplanted into sublethally irradiated recipient mice (Figure 2A). Mice transplanted with control MLL-ENL cells died of leukemia within 90 days, as is consistent with the previous report (Figure 2B).<sup>24</sup> Remarkably, leukemia onset was significantly earlier in mice transplanted with *Aml1*-excised MLL-ENL cells (*Aml1* <sup>$\Delta/\Delta$</sup> ; 49.5 ± 6 days vs *Aml1*<sup>fl/fl</sup>; 75 ± 9 days, *P* < .01). Immunophenotyping of leukemic cells revealed infiltration of Mac-1<sup>+</sup>/Sca1<sup>–</sup> cells, and Wright-Giemsa–stained peripheral blood smears showed immature blasts in both types of leukemia (Figure 2C; and data not shown). Surface marker expression, including c-Kit, Sca-1, Mac-1, and Gr-1, was not significantly changed regardless of *Aml1* status (Figure 2C).

### Induction of MLL-ENL leukemia after conditional deletion of AML1

A previous study shows that MLL-ENL leukemia can arise from hematopoietic stem cells (HSCs), common myeloid progenitors (CMPs),

and granulocyte-macrophage progenitors (GMPs), whereas transfection efficiency is higher in HSCs than in CMPs and GMPs.<sup>28</sup> In our previous experiment of MLL-ENL leukemia, we retrovirally introduced MLL-ENL into *Aml1*-excised BM cells. On the other hand, we have already reported that the number of HSCs is increased in *Aml1*-excised mice.<sup>19</sup> Because HSCs are increased in the *Aml1*-excised BM, there is one possibility that earlier onset of MLL-ENL leukemia from *Aml1*-excised BM cells is just the result of an increased number of MLL-ENL–transduced HSCs in the *Aml1*-excised BM. To explore this possibility, we transduced MLL-ENL into the BM cells from *Aml1*<sup>flox/flox</sup>; Mx-Cre(–) or *Aml1*<sup>flox/flox</sup>; Mx-Cre(+) before injection of pIpC. We transplanted those cells into sublethally irradiated recipient mice and injected pIpC one month after transplantation to delete *Aml1* in *Aml1*<sup>flox/flox</sup>; Mx-Cre(+) cells (Figure 3A). We found that the onset of leukemia from *Aml1*-excised cells (*Aml1* <sup>$\Delta/\Delta$</sup> ) was earlier than that of control cells (*Aml1*<sup>fl/fl</sup>; Figure 3B), indicating that loss of AML1 accelerates the development of leukemia even after introduction of MLL-ENL. These results suggest that the earlier onset of MLL-ENL leukemia from *Aml1*-excised hematopoietic progenitors is not simply the result of an increase in immature cells that can be efficiently transformed by MLL-ENL but potentially caused by an enhanced leukemogenic potential of MLL-ENL–transduced cells.

### AML1 deletion in MLL-ENL mice does not increase leukemia-initiating cells

Next, we performed limiting dilution analysis to estimate the frequency of leukemia-initiating cells (LICs) of MLL-ENL leukemia in these murine models. Twenty to 500 000 MLL-ENL leukemic cells harvested from recipient mice were transplanted into sublethally irradiated secondary recipient mice (Figure 2A). As shown in Table 1, 500 leukemic cells were sufficient to induce leukemia in all secondary recipient mice, regardless of the status of *Aml1*. Moreover, the incidence of leukemia in the recipient mice injected with 20 *Aml1*-excised leukemic cells was not significantly changed. These results indicate that the frequency of LICs is not altered in *Aml1*-excised MLL-ENL leukemic cells and that the early onset of MLL-ENL leukemia is not the result of an increased number of LICs.

### Decreased expression of cell cycle– and apoptosis-related genes in *Aml1*-excised leukemic cells

Given that the number of LICs is not significantly altered in *Aml1*-excised MLL-ENL leukemic cells, we evaluated the correlation between *Aml1* status and proliferative potentials of MLL-ENL leukemic cells. As shown in Figure 4A, the growth rate of *Aml1*-excised MLL-ENL cells obtained from the leukemic mice culture was enhanced in liquid compared with that of *Aml1*-intact MLL-ENL cells, as is consistent with the proliferation of the in vitro transformed cells (Figure 1E). To explore the mechanism of the growth advantage of MLL-ENL leukemic cells in the absence of AML1, we analyzed cell-cycle status and apoptotic rate of *Aml1*-excised MLL-ENL leukemic cells. Cell-cycle analyses revealed a significant increase of S/G<sub>2</sub>/M phase cells in *Aml1*-excised MLL-ENL leukemic cells (Figure 4B-C). Moreover, the rate of annexin V-positive apoptotic cells was reduced in *Aml1*-excised MLL-ENL leukemic cells in liquid culture with and without IL-3 (Figure 4D). These results suggest that

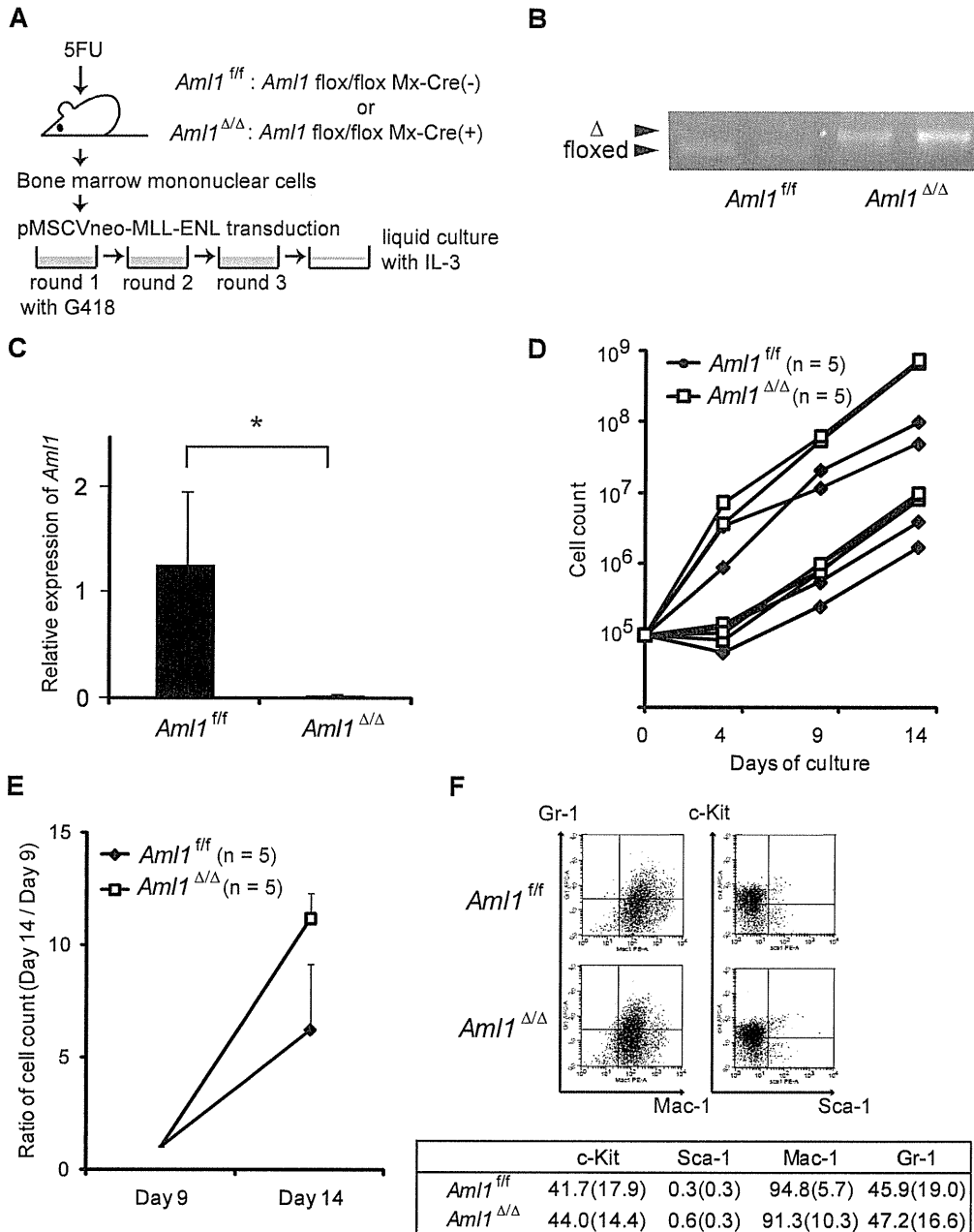


**Figure 1. Proliferation of *Aml1*-excised immortalized BM cells is enhanced in vitro.** (A) MLL-ENL was retrovirally transduced into *Aml1* intact (*Aml1*<sup>fl/fl</sup>) and excised (*Aml1*<sup>Δ/Δ</sup>) BM cells, and replating assay was performed using these cells. (B) Genotyping of *Aml1* floxed and Δ alleles by PCR from *Aml1*<sup>fl/fl</sup> and *Aml1*<sup>Δ/Δ</sup> immortalized cells. Each lane indicates the PCR products of an independent case. (C) mRNA levels of *Aml1* in *Aml1*<sup>fl/fl</sup> and *Aml1*<sup>Δ/Δ</sup> immortalized cells were measured. \**P* < .05. (D) Growth of *Aml1*<sup>fl/fl</sup> (n = 5; ◆) or *Aml1*<sup>Δ/Δ</sup> (n = 5; □) immortalized cells in liquid medium. Data are on a semilogarithmic plot of cell counts versus time. (E) Growth of the immortalized cells as in Figure 1D after day 9. Cell counts at day 14 relative to those at day 9 are shown as mean ± SD on a linear plot (n = 5 from each group). Day 14 proliferation was significantly different between groups (*t* test, *P* < .001). (F) Flow cytometric analyses of the colony-forming cells after 3 rounds of replating. (Top) Representative fluorescence-activated cell sorter plots. (Bottom) Percentages of cells expressing indicated surface markers in each group (mean ± SD).

growth advantage of *Aml1*-excised MLL-ENL leukemic cells depends on both acceleration of cell-cycle progression and inhibition of apoptosis. Consistently, expression of cell cycle-regulating genes, such as *p19<sup>ARF</sup>* and *p21<sup>CIP1</sup>*, decreased in *Aml1*-excised leukemic cells (Figure 5A). Expression of apoptosis-related genes, such as *p53* and *Bax*, also decreased in those cells (Figure 5A). On flow cytometric analysis, we observed that *Aml1*-excised leukemic cells expressed lesser amount of p53 protein (Figure 5B). The geometric mean fluorescence intensity

and SD of p53–AlexaFluor-647 was  $9.7 \pm 1.3$  for *Aml1*-excised cells and  $14.2 \pm 2.0$  for controls (*P* = .030). In contrast, expression of *Meis1* and *Hoxa* (*Hoxa5*, *Hoxa7*, *Hoxa9*, and *Hoxa10*), which are direct target genes of MLL-ENL,<sup>29</sup> was not changed in *Aml1*-excised MLL-ENL cells compared with controls (Figure 5C).

It was reported that loss of AML1 in mouse BM cells induces the enhanced expression of the Polycomb gene *Bmi-1* and an increase in the stem/progenitor cells because of suppression of

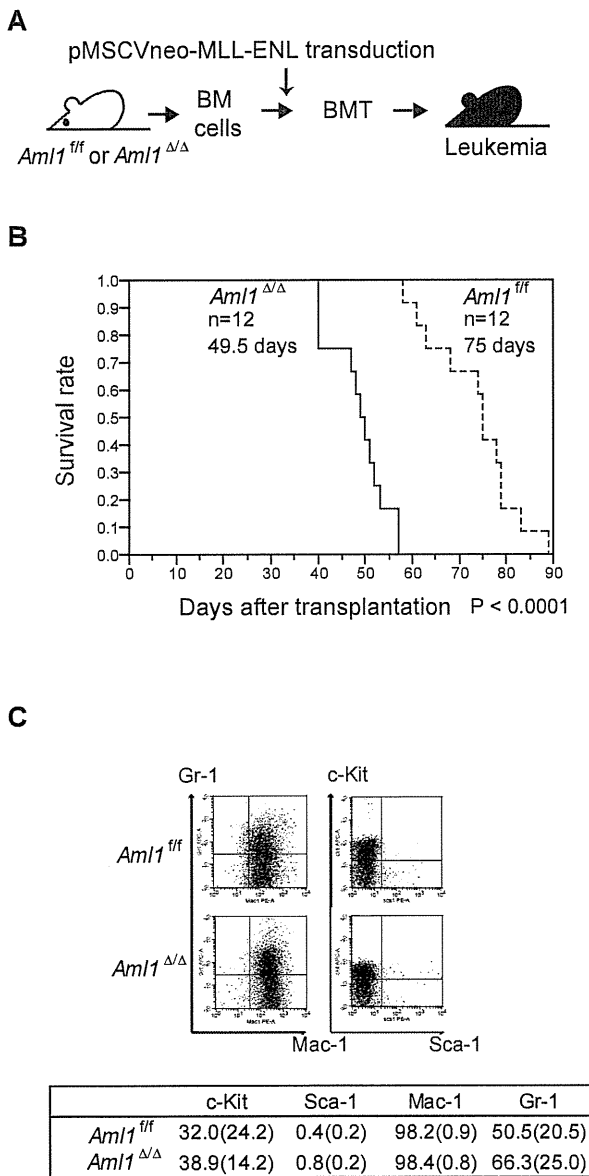


**Figure 2. Earlier onset of *Aml1*-excised MLL-ENL leukemia.** (A) BM cells from *Aml1*<sup>fl/fl</sup> and *Aml1*<sup>Δ/Δ</sup> mice were transduced with MLL-ENL and transplanted into congenic mice. (B) Survival curves of the mice transplanted with *Aml1*<sup>fl/fl</sup> and *Aml1*<sup>Δ/Δ</sup> cells transduced with MLL-ENL. Data from 12 mice for each group are shown. Comparison of survival curve was performed using log-rank test. (C) Flow cytometric analyses of the leukemic cells from transplanted mice. (Top) Representative fluorescence-activated cell sorter plots. (Bottom) Percentages of cells expressing indicated surface markers in each group (mean ± SD).

apoptosis.<sup>30</sup> *Bmi-1*, which is highly expressed in HSCs, critically suppresses the expression of *p19*<sup>ARF</sup> and *p16*<sup>INK4a</sup> in the regulation of hematopoietic cell proliferation.<sup>31</sup> Therefore, down-regulation of *p19*<sup>ARF</sup> may be a consequence of *Bmi-1* up-regulation by loss of AML1. To explore this possibility, we determined the expression of *Bmi-1* in *Aml1*-excised MLL-ENL-transduced cells and found that there was no significant change in *Bmi-1* expression, suggesting that *p19*<sup>ARF</sup> down-regulation is independent of *Bmi-1*. Consistently, the expression of *p16*<sup>INK4a</sup>, another target gene of *Bmi-1*, is also unaffected by loss of AML1 (Figure 5D).

### Transcriptional regulation of *p19*<sup>ARF</sup> by AML1 in MLL-ENL leukemic cells

It has been reported that overexpression of AML1 up-regulates the expression of *P14*<sup>ARF</sup> (human homolog of murine *p19*<sup>ARF</sup>), whereas AML1-ETO, a chimeric protein that exerts a dominant-negative effect over normal AML1, down-regulates its expression by directly binding to the promoter.<sup>20</sup> Because *p19*<sup>ARF</sup> affects cell cycle and apoptosis by regulating p53, Bax, and p21<sup>CIP1</sup>, we hypothesized that *p19*<sup>ARF</sup> is a critical effector in the AML1-mediated regulation of MLL-ENL leukemia. To test this, we expressed AML1 in *Aml1*-excised MLL-ENL leukemic cells and evaluated whether *p19*<sup>ARF</sup> is expressed in an AML1 dose-dependent manner. We collected MLL-ENL leukemic cells and transduced them with AML1. Forty-eight hours after transduction, we assessed the expression of *p19*<sup>ARF</sup> in these cells by real-time reverse-transcribed PCR. As shown in Figure 6A, overexpression of AML1 enhanced *p19*<sup>ARF</sup> expression in *Aml1* intact MLL-ENL-transformed cells. Expression of *p19*<sup>ARF</sup> in *Aml1*-excised MLL-ENL cells is decreased compared with controls, and this reduction was rescued by restoration of AML1 to the level observed in *Aml1* intact cells transduced with GFP (Figure 6A). *p19*<sup>ARF</sup> expression levels in this setting were higher than the results of primary leukemic cells (Figure 5A), probably because of additional retroviral transduction and in vitro culture. These results are consistent with the hypothesis that AML1 up-regulates the expression of *p19*<sup>ARF</sup> also in MLL-ENL leukemia.

To determine a role of *p19*<sup>ARF</sup> in MLL-ENL leukemia in vivo, we tested whether down-regulation of *p19*<sup>ARF</sup> can accelerate the onset of MLL-ENL leukemia. We used short hairpin RNA (shRNA) to knock down the expression of *p19*<sup>ARF</sup>.<sup>25</sup> We retrovirally transduced 3000 MLL-ENL leukemic cells with 2 types of *p19*<sup>ARF</sup>-directed shRNAs and injected them into sublethally irradiated secondary recipient mice. As shown in Figure 6B, only 42% of mice injected with leukemic cells transduced with control shRNAs developed leukemia. On the other hand, nearly all mice injected with leukemic cells transduced with *p19*<sup>ARF</sup> shRNAs developed leukemia in shorter latencies. *p19*<sup>ARF</sup> expression levels in cells of secondary leukemic mice were lower than those in primary leukemic mice (Figures 5A, 6C), possibly because of the development of secondary leukemia in vivo. We confirmed that expression of *p19*<sup>ARF</sup> was efficiently suppressed in leukemic cells obtained from *p19*<sup>ARF</sup> shRNAs-transduced MLL-ENL mice (Figure 6C). These results indicate that *p19*<sup>ARF</sup> down-regulation promotes the development of MLL-ENL leukemia, which supports the notion that *p19*<sup>ARF</sup> plays a critical role in the acceleration of MLL-ENL leukemia induced by loss of AML1.

To examine the direct binding of AML1 to the *p19*<sup>ARF</sup> promoter, we performed chromatin immunoprecipitation assays. Two consensus AML1 binding sites (PEBP2 sites) were found in the *p19*<sup>ARF</sup> promoter (Figure 6D). The splenocytes from MLL-ENL leukemic mice were lysed after crosslinking by formaldehyde and eluted DNA was broken by sonication. Protein-DNA complexes were immunoprecipitated by the anti-AML1 antibody or normal rabbit IgG. Then we amplified the genomic DNA from this solution using the primers for the sequence containing the PEBP2 sites and found that the distal PEBP2 site of *p19*<sup>ARF</sup> promoter was significantly coprecipitated with AML1, suggesting that AML1 binds to the *p19*<sup>ARF</sup> promoter (Figure 6E). To ascertain whether the distal PEBP2 site contributes to AML1-dependent transactivation of the *p19*<sup>ARF</sup> promoter, we performed a luciferase reporter assay. We

A

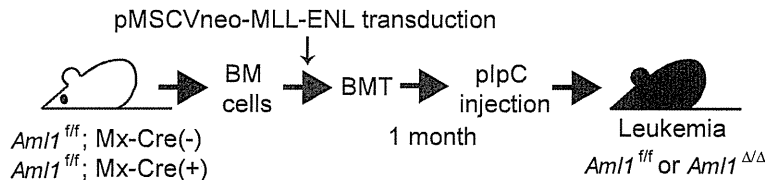
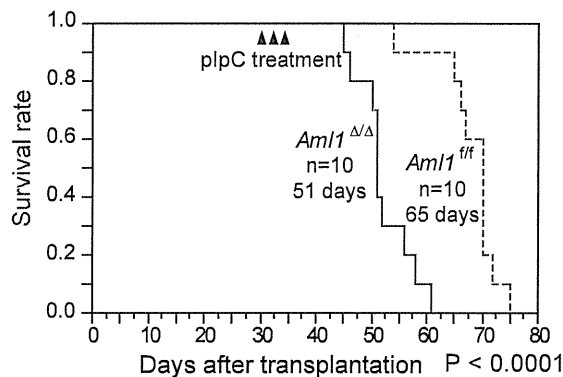


**Figure 3. Deletion of the AML1 gene after MLL-ENL induction accelerates the onset of leukemia in transplanted mice.** (A) BM cells from *Aml1*<sup>flf</sup>; Mx-Cre (+) or *Aml1*<sup>flf</sup>; Mx-Cre (-) were transduced with MLL-ENL and transplanted into congenic mice. Injection with plpC was performed 3 to 4 weeks after transplantation, so that the *Aml1* gene was excised in transplanted *Aml1*<sup>flf</sup>; Mx-Cre (+) cells (*Aml1*<sup>ΔΔ</sup>). (B) Survival curves of the recipient mice. Data from 10 mice for each group are shown. Arrowheads indicate plpC injection. Comparison of survival curve was performed using log-rank test.

B



constructed a luciferase reporter containing the 0.6-kb fragment of the *p19<sup>ARF</sup>* promoter, and a mutant reporter containing the same promoter fragment in which the distal PEBP2 site (CGCGGT) was mutated (TTTTTT). COS-7 cells were cotransfected with an AML1 expression plasmid and these luciferase reporter plasmids. As shown in Figure 6F, AML1 activated the *p19<sup>ARF</sup>* promoter > 2-fold, whereas *p19<sup>ARF</sup>*-mutated promoter was not activated by AML1. These results indicate that AML1 regulates *p19<sup>ARF</sup>* transcription through binding to the distal PEBP2 site.

## Discussion

The results presented here provide direct evidence that loss of AML1 induces the accelerated onset of MLL-ENL leukemia in mice because of enhanced proliferation of leukemic cells. Because additional mutations are required for the development of full-blown leukemia along with loss of AML1 function, their cooperation in leukemogenesis is of interest in understanding the molecular mechanisms of human leukemia. Recently, coexistence of *MLL-PTD* mutation and *AML1* point mutation in

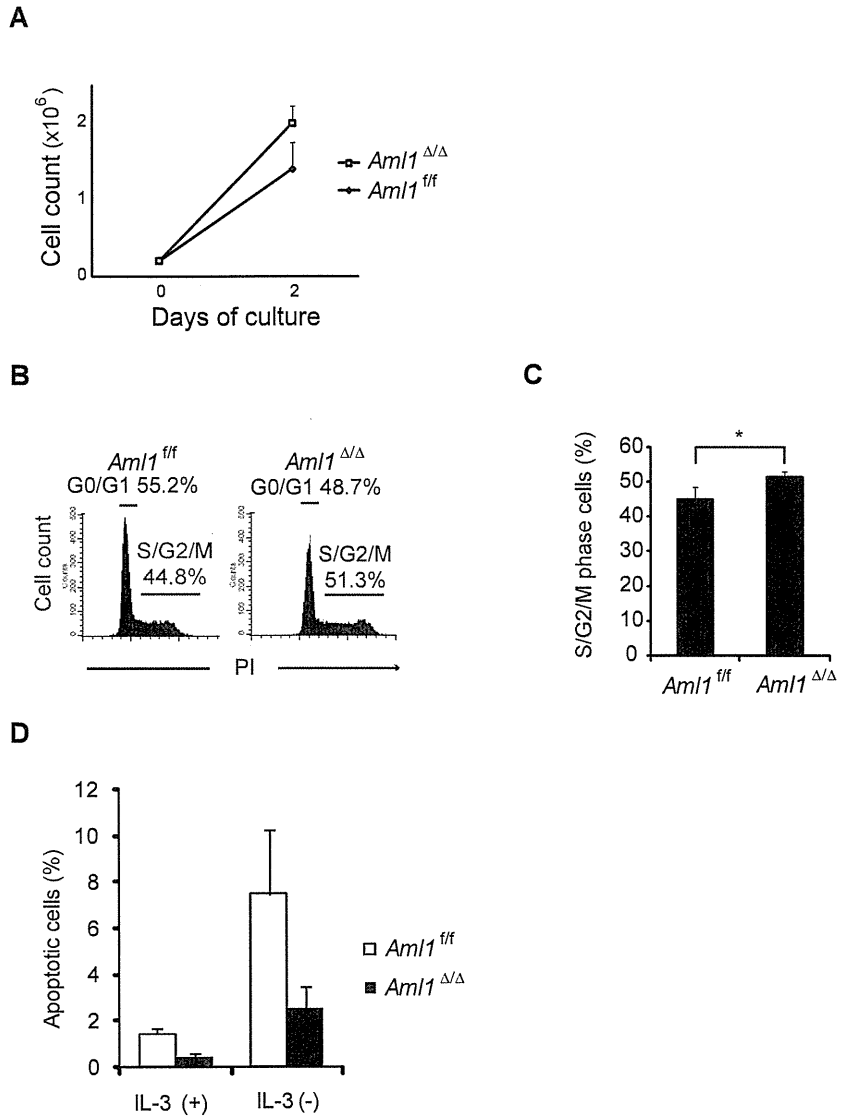
AML with normal karyotype was reported,<sup>17</sup> and the significance of this correlation in leukemogenesis is to be elucidated. In this regard, to understand the interaction between *AML1* mutation and MLL leukemia, we explored accelerated leukemogenesis in *Aml1*-excised cells in vitro and in vivo using MLL-ENL fusion-induced mouse AML model. Our results indicate that AML1 acts as a tumor suppressor against the *MLL-ENL* oncogene, and loss of AML1 supports the development of leukemia via down-regulation of the genes related to the cell-cycle inhibition and apoptosis. Among them is *p19<sup>ARF</sup>*, which acts as a negative regulator of cellular proliferation upstream of the cascade, including p53 and p21<sup>CIP1</sup>. We found that AML1 activates transcription of *p19<sup>ARF</sup>* in MLL-ENL leukemic cells mainly through binding to distal consensus AML1 binding site (PEBP2 site) in the *p19<sup>ARF</sup>* promoter (Figure 6D) and that down-regulation of *p19<sup>ARF</sup>* induces the early onset of MLL-ENL leukemia, suggesting that *p19<sup>ARF</sup>* is a major target of AML1 in MLL-ENL leukemia (Figure 6A-B). These results suggest the function of AML1 as a tumor suppressor. Supporting our observation with the mouse model, down-regulation of *p14<sup>ARF</sup>*, a human homolog of mouse *p19<sup>ARF</sup>*, has also been reported in patients with human AML1-ETO leukemia.<sup>20</sup> Several other mutations, such as *ASXL1*<sup>32</sup> and *FLT3*<sup>33</sup> mutations, are reported in AML with point mutations of *AML1*, and our results suggest a novel mechanistic basis also for these leukemias.

Motoda et al reported that loss of AML1 in mouse BM cells induces the enhanced expression of Bmi-1 and an increase in hematopoietic stem/progenitor cells because of suppression of apoptosis.<sup>30</sup> They demonstrated that *p19<sup>ARF</sup>* expression was decreased in AML1-deficient BM cells and that the enhanced expression of *p19<sup>ARF</sup>* by *N-Ras* mutation was also decreased by

**Table 1. Quantification of leukemia initiating cells**

No. of transplanted cells	No. of leukemic mice/no. of transplanted mice	
	<i>Aml1</i> <sup>flf</sup> MLL-ENL cells	<i>Aml1</i> <sup>ΔΔ</sup> MLL-ENL cells
500 000	8/8	8/8
50 000	8/8	8/8
5000	8/8	8/8
500	8/8	8/8
20	5/8	4/8

**Figure 4. Aml1-excised MLL-ENL leukemic cells revealed accelerated growth rate because of enhanced cell-cycle progression and inhibition of apoptosis.** (A) Growth rate of *Aml1*-excised leukemic cells in liquid medium was compared with controls. Data are mean  $\pm$  SD. (B-C) Cell-cycle analyses of leukemic cells by PI. (B) Representative histograms are shown. (C) Percentages of cells in S/G<sub>2</sub>/M phase (mean  $\pm$  SD). (D) Percentages of apoptotic cells in each liquid medium (mean  $\pm$  SD). \**P* < .05. We performed 3 independent experiments and confirmed that similar results were reproduced. Statistical significance was evaluated by unpaired *t* test.



loss of AML1. In their study, it is suggested that *N-Ras* mutation directly activates p19<sup>ARF</sup> and that AML1 indirectly induces the expression of p19<sup>ARF</sup> via down-regulation of Bmi-1. However, we found that the expression level of Bmi-1 is not changed by loss of AML1 in MLL-ENL leukemic cells and that p19<sup>ARF</sup> is directly regulated by AML1 (Figures 5D, 6E-F). Therefore, different molecular mechanisms that cooperate with loss of AML1 may exist in MLL-ENL and N-Ras leukemias, which remain to be elucidated.

In our study, we found that the expression level of *p53* gene is also decreased in *Aml1*-excised MLL-ENL leukemic cells (Figure 5A). These cells expressed significantly less amount of p53 protein (Figure 5B). Therefore, loss of p53 is probably involved in the enhanced proliferation of AML1-deficient MLL-ENL leukemic cells, supporting our notion that the p19<sup>ARF</sup>-MDM2-p53 pathway may play a critical role in the acceleration of MLL-ENL leukemia induced by loss of AML1. However, it is well known that p19<sup>ARF</sup> blocks p53 degradation by binding to MDM2,<sup>34,35</sup> and regulation of p53 transcription by p19<sup>ARF</sup> has not been reported. We confirmed that the expression

levels of p53 did not increase in MLL-ENL leukemic cells by overexpression of p19<sup>ARF</sup> (data not shown). Therefore, it remains to be elucidated which of transcriptional regulation and posttranslational regulation is more important than the other for the reduction of p53 protein.

HSCs and LICs share several biologic properties, such as self-renewal capacities and an ability to differentiate into more differentiated cells. These similarities have led us to hypothesize that the number of LICs may be increased in *Aml1*-excised MLL-ENL leukemic cells as a consequence of HSC expansion by loss of AML1.<sup>36-42</sup> However, the number of LICs was not affected by loss of AML1 in MLL-ENL mice, suggesting that promotion of MLL-related leukemia by loss of AML1 is not the result of the expansion of target population for leukemic transformation but mainly derived from the enhanced proliferation of MLL-ENL leukemic cells (Table 1). Given that MLL-ENL provides self-renewal capacities to the myeloid progenitors, including CMPs and GMPs, which are normally incapable of self-renewal,<sup>28</sup> HSC expansion caused by loss of AML1 may not influence MLL-related leukemogenesis.

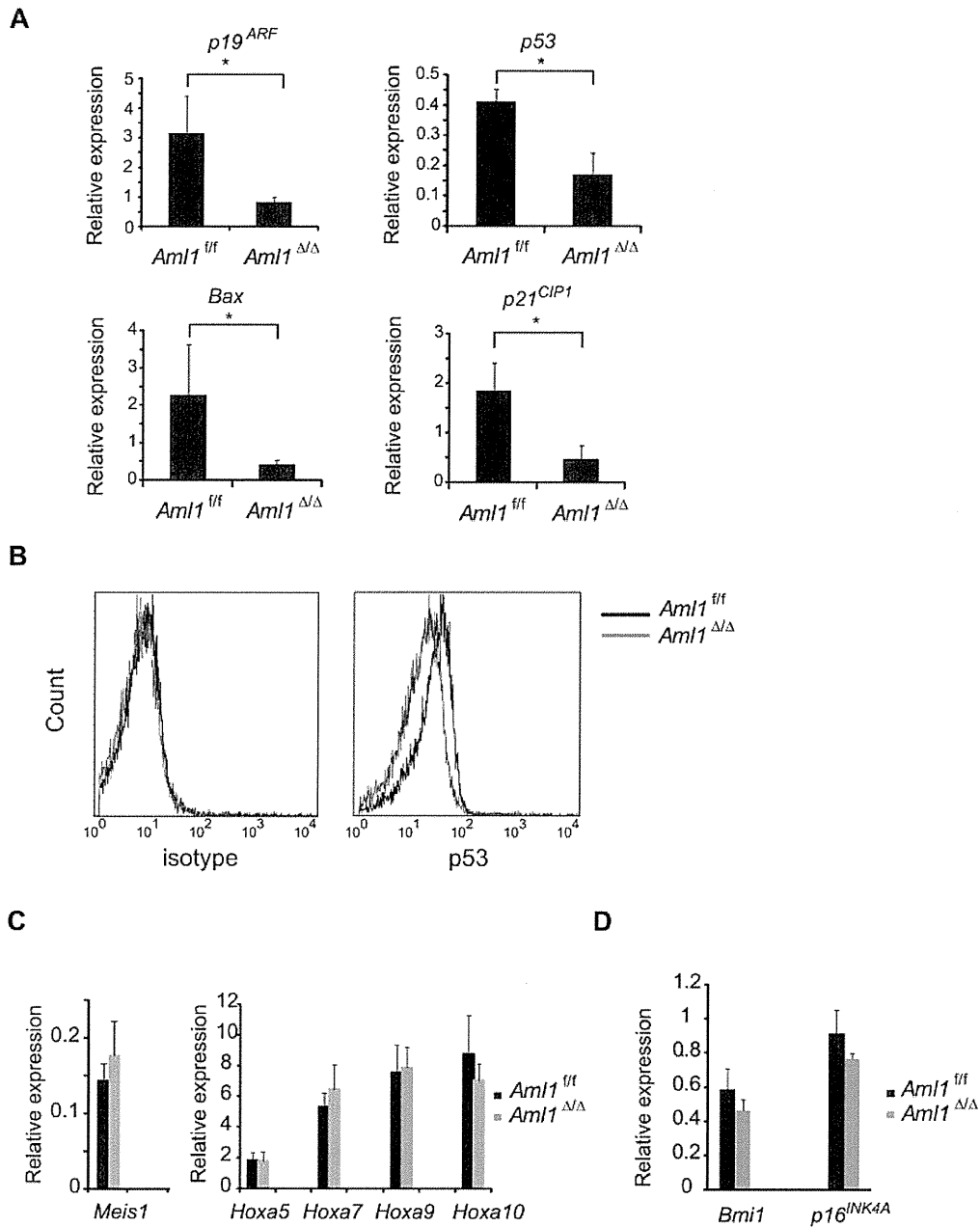


**Figure 5. Decreased expression of cell cycle- and apoptosis-related genes in *Aml1*-excised leukemia cell.** (A) Expression analyses of *p19<sup>ARF</sup>*, *p53*, *Bax*, and *p21<sup>CIP1</sup>* by quantitative real-time PCR. The expression of each mRNA, normalized to that of *Gapdh*, is shown as the ratio to that of the normal BM mononuclear cells. (B) Intracellular staining of p53 in MLL-ENL leukemic cells was detected by flow cytometry. Representative histograms are shown. (Left) Staining with AlexaFluor-647-conjugated IgG1 isotype control antibodies. (Right) Staining with AlexaFluor-647-conjugated anti-p53 antibodies. Expression analyses of (C) *Meis1* and *Hoxa* genes and (D) *Bmi1* and *p16<sup>INK4A</sup>* by quantitative real-time PCR. Error bars represent SD. \**P* < .05. We performed 3 independent experiments and confirmed that similar results were reproduced. Statistical significance was evaluated by unpaired *t* test.

*Aml1*-excised transformed cells developed MLL-ENL leukemia earlier than *Aml1* intact cells (Figures 2B, 3B). When *Aml1* was excised from the MLL-ENL-transduced cells after engraftment in the individual mice, transplanted mice developed leukemia in as early as 21 days (Figure 3B); in contrast, the mice transplanted with MLL-ENL-transduced, *Aml1*-excised cells developed leukemia in 49.5 days after transplantation (Figure 2B). This may be because the transplanted cells in Figure 3B had already expanded and progressed to the leukemic or preleukemic state by MLL-ENL at

the time of *Aml1* excision and the *Aml1* excision caused enhanced proliferation of the leukemic cells to shorten the latency to develop leukemia (Figure 3B).

Our study is the first report to reveal the molecular mechanism of leukemia acceleration caused by loss of AML1. Our results demonstrate that p19<sup>ARF</sup> is a key molecule for the proliferation of leukemic cells in AML1-related leukemia. Targeted therapy for aberrant p19<sup>ARF</sup> signaling pathway may be a novel therapeutic strategy against AML1-related leukemia.



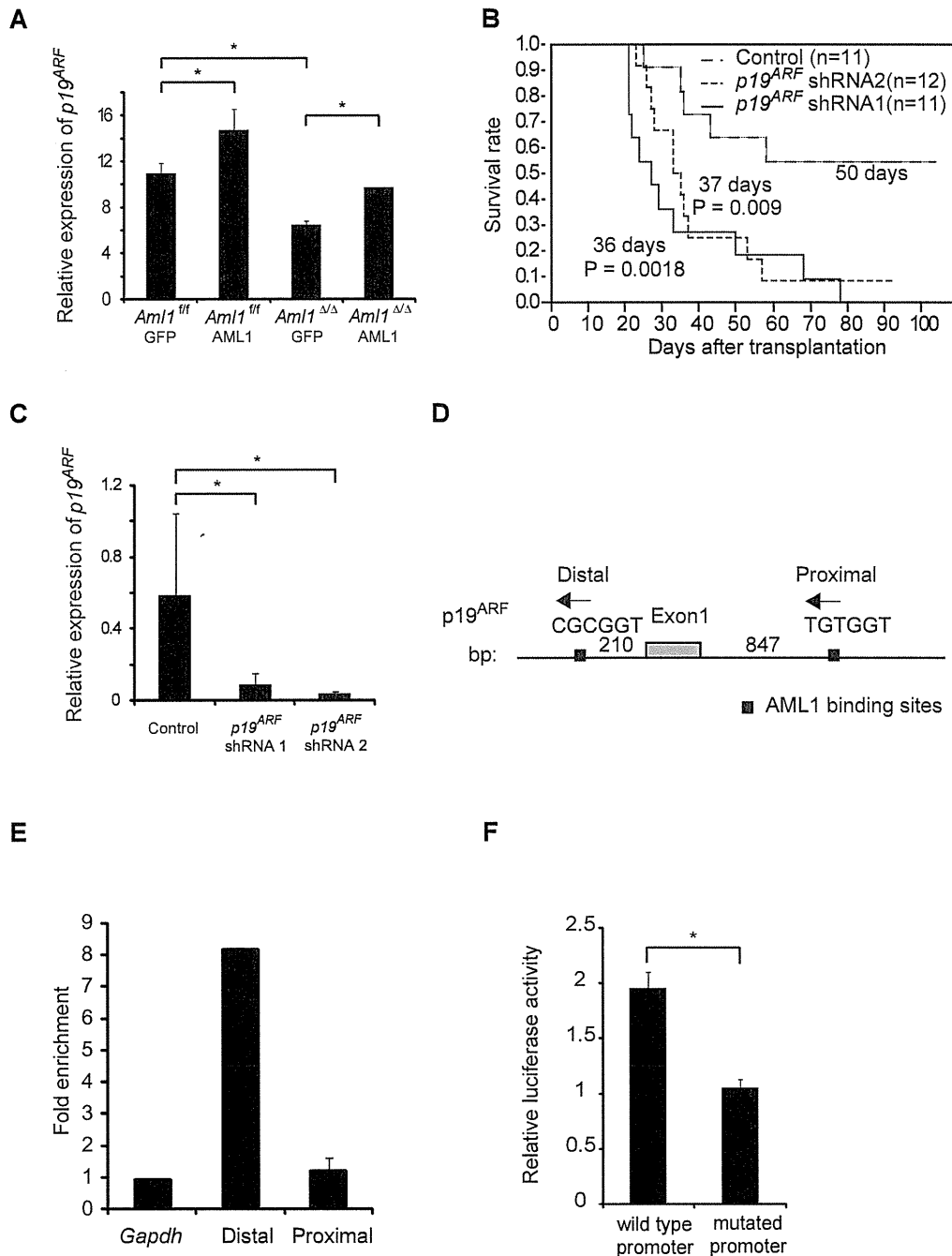


**Figure 6. Expression of *p19<sup>ARF</sup>* is regulated by AML1 in MLL-ENL leukemia.** (A) Expression analyses of *p19<sup>ARF</sup>* in MLL-ENL leukemic cells. *Aml1* intact or *Aml1*-excised MLL-ENL leukemic cells harvested from each spleen were transduced with GFP or AML1-GFP. Forty-eight hours later, expression levels of *p19<sup>ARF</sup>* were measured by quantitative real-time PCR. (B) *Aml1* intact MLL-ENL leukemic cells were transduced with *p19<sup>ARF</sup>* shRNA or control shRNA and transplanted into secondary recipient mice. Survival curves of 12 mice from each group are shown. Comparison of survival curve was performed using log-rank test. (C) Expression levels of *p19<sup>ARF</sup>* in leukemic cells from secondary recipient mice were measured by quantitative real-time PCR. (D) Two AML1 binding sites located in the promoter of *p19<sup>ARF</sup>* are shown as indicated. (E) Chromatin immunoprecipitation analyses of AML1 for *p19<sup>ARF</sup>* promoter region in MLL-ENL leukemic cells. Fold enrichment normalized to the control locus *Gapdh* was shown. (F) COS7 cells were cotransfected with expression vector for AML1 and wild-type or PEBP2-site mutated *p19<sup>ARF</sup>* promoter vector. The relative luciferase activity was calculated as the ratio of luciferase activity with AML1 expression to that without AML1 expression. All luciferase reporter assays were performed in duplicate in 2 independent experiments. Values and error bars represent the mean and the SD, respectively. \**P* < .05. We performed 3 independent experiments and confirmed that similar results were reproduced, except for panel B. Statistical significance was evaluated by unpaired *t* test.

## Acknowledgments

The authors thank Dr S. W. Hiebert (Vanderbilt University, Nashville, TN), Dr H. Nakauchi (IMS, Tokyo University,

Tokyo, Japan), Dr T. Kitamura (IMS, Tokyo University, Tokyo, Japan), and Dr T. Nosaka (Mie University, Mie, Japan) for providing essential materials and instruments and M. Kobayashi, Y. Sawamoto, and Y. Shimamura for expert technical assistance.

This work was supported in part by the Ministry of Education, Culture, Sports, Science and Technology (grant KAKENHI 20790670).

## Authorship

Contribution: N.N., Y.I., M.N., M.I., and M.K. designed the experiments and the study; N.N., S.A., Y.I., M.N., S.G., K.K., T.T., Y.K., M.I., and M.K. wrote the manuscript; N.N., S.A., Y.I.,

M.N., and M.I. performed experiments and collected and analyzed data; S.G., K.K., and T.T. provided technical advice and support; and M.K. supervised all of the experiments and data interpretation.

Conflict-of-interest disclosure: The authors declare no competing financial interests.

Correspondence: Mineo Kurokawa, Department of Hematology and Oncology, Graduate School of Medicine, University of Tokyo, 7-3-1 Hongo, Bunkyo-ku, Tokyo, Japan 113-8655; e-mail: kurokawa-tyk@umin.ac.jp.

## References

- Miyoshi H, Shimizu K, Kozu T, Maseki N, Kaneko Y, Ohki M. t(8;21) breakpoints on chromosome 21 in acute myeloid leukemia are clustered within a limited region of a single gene, AML1. *Proc Natl Acad Sci U S A*. 1991;88(23):10431-10434.
- Lutterbach B, Hiebert SW. Role of the transcription factor AML-1 in acute leukemia and hematopoietic differentiation. *Gene*. 2000;245(2):223-235.
- Marcucci G, Caligiuri MA, Bloomfield CD. Molecular and clinical advances in core binding factor primary acute myeloid leukemia: a paradigm for translational research in malignant hematology. *Cancer Invest*. 2000;18(8):768-780.
- Peterson LF, Zhang DE. The 8;21 translocation in leukemogenesis. *Oncogene*. 2004;23(24):4255-4262.
- Okuda T, van Deursen J, Hiebert SW, Grosveld G, Downing JR. AML1, the target of multiple chromosomal translocations in human leukemia, is essential for normal fetal liver hematopoiesis. *Cell*. 1996;84(2):321-330.
- Ichikawa M, Asai T, Saito T, et al. AML-1 is required for megakaryocytic maturation and lymphocytic differentiation, but not for maintenance of hematopoietic stem cells in adult hematopoiesis. *Nat Med*. 2004;10(3):299-304.
- Imai Y, Kurokawa M, Izutsu K, et al. Mutations of the AML1 gene in myelodysplastic syndrome and their functional implications in leukemogenesis. *Blood*. 2000;96(9):3154-3160.
- Osato M, Asou N, Abdalla E, et al. Biallelic and heterozygous point mutations in the runt domain of the AML1/PEBP2alphaB gene associated with myeloblastic leukemias. *Blood*. 1999;93(6):1817-1824.
- Song WJ, Sullivan MG, Legare RD, et al. Haploinsufficiency of CBFA2 causes familial thrombocytopenia with propensity to develop acute myelogenous leukaemia. *Nat Genet*. 1999;23(2):166-175.
- de Guzman CG, Warren AJ, Zhang Z, et al. Hematopoietic stem cell expansion and distinct myeloid developmental abnormalities in a murine model of the AML1-ETO translocation. *Mol Cell Biol*. 2002;22(15):5506-5517.
- Fenske TS, Pengue G, Mathews V, et al. Stem cell expression of the AML1/ETO fusion protein induces a myeloproliferative disorder in mice. *Proc Natl Acad Sci U S A*. 2004;101(42):15184-15189.
- Higuchi M, O'Brien D, Kumaravelu P, Lenny N, Yeoh EJ, Downing JR. Expression of a conditional AML1-ETO oncogene bypasses embryonic lethality and establishes a murine model of human t(8;21) acute myeloid leukemia. *Cancer Cell*. 2002;1(1):63-74.
- Schwieger M, Lohler J, Friel J, Scheller M, Horak I, Stocking C. AML1-ETO inhibits maturation of multiple lymphohematopoietic lineages and induces myeloblast transformation in synergy with ICSPB deficiency. *J Exp Med*. 2002;196(9):1227-1240.
- Yuan Y, Zhou L, Miyamoto T, et al. AML1-ETO expression is directly involved in the development of acute myeloid leukemia in the presence of additional mutations. *Proc Natl Acad Sci U S A*. 2001;98(18):10398-10403.
- Schessl C, Rawat VP, Cusan M, et al. The AML1-ETO fusion gene and the FLT3 length mutation collaborate in inducing acute leukemia in mice. *J Clin Invest*. 2005;115(8):2159-2168.
- Yamashita N, Osato M, Huang L, et al. Haploinsufficiency of Runx1/AML1 promotes myeloid features and leukaemogenesis in BXH2 mice. *Br J Haematol*. 2005;131(4):495-507.
- Tang J, Hou H, Chen C, et al. AML1/RUNX1 mutations in 470 adult patients with de novo acute myeloid leukemia: prognostic implication and interaction with other gene alterations. *Blood*. 2009;114(26):5352-5361.
- Wang YY, Zhou GB, Yin T, et al. AML1-ETO and C-KIT mutation/overexpression in t(8;21) leukemia: implication in stepwise leukemogenesis and response to Gleevec. *Proc Natl Acad Sci U S A*. 2005;102(4):1104-1109.
- Ichikawa M, Goyama S, Asai T, et al. AML1/Runx1 negatively regulates quiescent hematopoietic stem cells in adult hematopoiesis. *J Immunol*. 2008;180(7):4402-4408.
- Linggi B, Muller-Tidow C, van de Locht L, et al. The t(8;21) fusion protein, AML1 ETO, specifically represses the transcription of the p14(ARF) tumor suppressor in acute myeloid leukemia. *Nat Med*. 2002;8(7):743-750.
- Ono R, Nakajima H, Ozaki K, et al. Dimerization of MLL fusion proteins and FLT3 activation synergize to induce multiple-lineage leukemogenesis. *J Clin Invest*. 2005;115(4):919-929.
- Goyama S, Yamaguchi Y, Imai Y, et al. The transcriptionally active form of AML1 is required for hematopoietic rescue of the AML1-deficient embryonic para-aortic splanchnopleural (P-Sp) region. *Blood*. 2004;104(12):3558-3564.
- Kitamura T, Koshino Y, Shibata F, et al. Retrovirus-mediated gene transfer and expression cloning: powerful tools in functional genomics. *Exp Hematol*. 2003;31(11):1007-1014.
- Kawazu M, Asai T, Ichikawa M, et al. Functional domains of Runx1 are differentially required for CD4 repression, TCRbeta expression, and CD4/8 double-negative to CD4/8 double-positive transition in thymocyte development. *J Immunol*. 2005;174(6):3526-3533.
- Liu Y, Chen L, Ko TC, Fields AP, Thompson EA. Evi1 is a survival factor which conveys resistance to both TGFbeta- and taxol-mediated cell death via PI3K/AKT. *Oncogene*. 2006;25(25):3565-3575.
- Shimabe M, Goyama S, Watanabe-Okochi N, et al. Pbx1 is a downstream target of Evi-1 in hematopoietic stem/progenitors and leukemic cells. *Oncogene*. 2009;28(49):4364-4374.
- Lee TI, Johnstone SE, Young RA. Chromatin immunoprecipitation and microarray-based analysis of protein location. *Nat Protoc*. 2006;1(2):729-748.
- Cozzio A, Passegue E, Ayton PM, Karsunky H, Cleary ML, Weissman IL. Similar MLL-associated leukemias arising from self-renewing stem cells and short-lived myeloid progenitors. *Genes Dev*. 2003;17(24):3029-3035.
- Yokoyama A, Cleary ML. Menin critically links MLL proteins with LEDGF on cancer-associated target genes. *Cancer Cell*. 2008;14(1):36-46.
- Motoda L, Osato M, Yamashita N, et al. Runx1 protects hematopoietic stem/progenitor cells from oncogenic insult. *Stem Cells*. 2007;25(12):2976-2986.
- Jacobs JJ, Kieboom K, Marino S, DePinho RA, van Lohuizen M. The oncogene and Polycomb-group gene bmi-1 regulates cell proliferation and senescence through the ink4a locus. *Nature*. 1999;397(6715):164-168.
- Chou W, Huang H, Hou H, et al. Distinct clinical and biological features of de novo acute myeloid leukemia with additional sex comb-like 1 (ASXL1) mutations. *Blood*. 2010;116(20):4086-4094.
- Dicker F, Haeflrich C, Sundermann J, et al. Mutation analysis for RUNX1, MLL-PTD, FLT3-ITD, NPM1 and NRAS in 269 patients with MDS or secondary AML. *Leukemia*. 2010;24(8):1528-1532.
- Pomerantz J, Schreiber-Agus N, Liegeois NJ, et al. The Ink4a tumor suppressor gene product, p19Arf, interacts with MDM2 and neutralizes MDM2's inhibition of p53. *Cell*. 1998;92(6):713-723.
- Zhang Y, Xiong Y, Yarbrough WG. ARF promotes MDM2 degradation and stabilizes p53: ARF-INK4a locus deletion impairs both the Rb and p53 tumor suppression pathways. *Cell*. 1998;92(6):725-734.
- Bonnet D, Dick JE. Human acute myeloid leukemia is organized as a hierarchy that originates from a primitive hematopoietic cell. *Nat Med*. 1997;3(7):730-737.
- Hope KJ, Jin L, Dick JE. Acute myeloid leukemia originates from a hierarchy of leukemic stem cell classes that differ in self-renewal capacity. *Nat Immunol*. 2004;5(7):738-743.
- Huntly BJ, Gilliland DG. Leukaemia stem cells and the evolution of cancer-stem-cell research. *Nat Rev Cancer*. 2005;5(4):311-321.
- Kato Y, Iwama A, Tadokoro Y, et al. Selective activation of STAT5 unveils its role in stem cell self-renewal in normal and leukemic hematopoiesis. *J Exp Med*. 2005;202(1):169-179.
- Lessard J, Sauvageau G. Bmi-1 determines the proliferative capacity of normal and leukaemic stem cells. *Nature*. 2003;423(6937):255-260.
- Park IK, Qian D, Kiel M, et al. Bmi-1 is required for maintenance of adult self-renewing haematopoietic stem cells. *Nature*. 2003;423(6937):302-305.
- Reya T, Clevers H. Wnt signalling in stem cells and cancer. *Nature*. 2005;434(7035):843-850.

## Evi1 represses PTEN expression and activates PI3K/AKT/mTOR via interactions with polycomb proteins

Akihide Yoshimi,<sup>1</sup> Susumu Goyama,<sup>1</sup> Naoko Watanabe-Okochi,<sup>1</sup> Yumiko Yoshiki,<sup>1</sup> Yasuhiro Nannya,<sup>1</sup> Eriko Nitta,<sup>1</sup> Shunya Arai,<sup>1</sup> Tomohiko Sato,<sup>1</sup> Munetake Shimabe,<sup>1</sup> Masahiro Nakagawa,<sup>1</sup> Yoichi Imai,<sup>1</sup> Toshio Kitamura,<sup>2</sup> and Mineo Kurokawa<sup>1</sup>

<sup>1</sup>Department of Hematology and Oncology, Graduate School of Medicine, University of Tokyo, Tokyo, Japan; and <sup>2</sup>Division of Stem Cell Signaling, Institute of Medical Science, University of Tokyo, Tokyo, Japan

**Evi1 (ecotropic viral integration site 1) is essential for proliferation of hematopoietic stem cells and implicated in the development of myeloid disorders. Particularly, high Evi1 expression defines one of the largest clusters in acute myeloid leukemia and is significantly associated with extremely poor prognosis. However, mechanistic basis of Evi1-mediated leukemogenesis has not been fully elucidated. Here, we show that Evi1 directly represses phosphatase and tensin homologue deleted on chromosome 10 (PTEN)**

**transcription in the murine bone marrow, which leads to activation of AKT/mammalian target of rapamycin (mTOR) signaling. In a murine bone marrow transplantation model, Evi1 leukemia showed modestly increased sensitivity to an mTOR inhibitor rapamycin. Furthermore, we found that Evi1 binds to several polycomb group proteins and recruits polycomb repressive complexes for PTEN down-regulation, which shows a novel epigenetic mechanism of AKT/mTOR activation in leukemia. Expression analyses**

**and ChIP assays with human samples indicate that our findings in mice models are recapitulated in human leukemic cells. Dependence of Evi1-expressing leukemic cells on AKT/mTOR signaling provides the first example of targeted therapeutic modalities that suppress the leukemogenic activity of Evi1. The PTEN/AKT/mTOR signaling pathway and the Evi1-polycomb interaction can be promising therapeutic targets for leukemia with activated Evi1. (*Blood*. 2011;117(13):3617-3628)**

### Introduction

*Evi1* (ecotropic viral integration site 1) is a nuclear transcription factor that is indispensable for proliferation of hematopoietic stem cells (HSCs) both during embryogenesis and in the adult.<sup>1,2</sup> Aberrant expression of *Evi1* is implicated in the development of myeloid disorders, including acute myeloid leukemia (AML), myelodysplastic syndrome, and chronic myelogenous leukemia (CML).<sup>3-5</sup> High *Evi1* expression occurs in ~ 10% of cases of AML and genetically defines one of the largest clusters in AML.<sup>6</sup> The patients classified into this cluster show an extremely poor outcome.<sup>6,7</sup> *Evi1* possesses diverse functions as an oncoprotein, including suppression of transforming growth factor- $\beta$ -mediated growth inhibition,<sup>8</sup> negative regulation of the c-Jun N-terminal kinase pathway,<sup>9</sup> and stimulation of cell growth by activator protein-1 (*AP-1*).<sup>10</sup> Aberrant expression of *Evi1* affects hematopoietic differentiation in various lineages. Several groups reported that *Evi1* blocks myeloid differentiation.<sup>11-13</sup> *Evi1* also affects differentiation of erythroid and megakaryocytic cells.<sup>11,14-16</sup> In addition to its DNA-binding activity, *Evi1* has the potential to recruit diverse proteins for transcriptional regulation. We and others have identified several target genes that are activated by *Evi1*, including globin transcription factor 2 (*GATA2*)<sup>2,17</sup> and pre-B-cell leukemia homeobox 1 (*PBX1*).<sup>18</sup> However, there are no reports of genes that are directly repressed by *Evi1*, despite that *Evi1* interacts with several transcriptional corepressors, such as C-terminal binding protein (CtBP),<sup>19</sup> SUV39H1, and G9a.<sup>20-22</sup>

Phosphatase and tensin homologue deleted on chromosome 10 (*PTEN*) plays critical roles in cell growth, migration, and death.<sup>23</sup> It is mutated or deleted with high frequency in various human cancer tissues to promote tumorigenesis.<sup>24</sup> The primary target of *PTEN* in cancer is phosphatidylinositol 3,4,5-triphosphate,<sup>25</sup> and the loss of *PTEN* leads to constitutively high expression of phosphatidylinositol 3,4,5-triphosphate, which induces AKT kinase activation.<sup>26</sup> AKT, in turn, phosphorylates a plethora of targets. In particular, AKT has a remarkable effect on cellular growth by activating the mammalian target of rapamycin (mTOR). Deletion of *PTEN* in murine adult HSCs has been studied by 2 groups.<sup>27,28</sup> Both groups observed the rapid onset of myeloproliferative disorders within 4-6 weeks after *PTEN* knockout, which rapidly progressed to acute leukemia. Importantly, these phenotypes could be rescued by mTOR inhibitor rapamycin.<sup>27</sup>

Epigenetic perturbations such as altered DNA methylation, misregulation of chromatin remodeling by histone modifications have emerged as common hallmarks of tumors.<sup>29,30</sup> Polycomb group (PcG) proteins are one of such epigenetic regulators. PcG proteins catalyze the addition of a methyl group at lysine 27 of histone H3 (H3K27me) and function as transcriptional regulators that silence specific sets of genes through chromatin modification.<sup>31,32</sup> PcG proteins comprise 2 functionally and biochemically distinct multimeric polycomb repressive complexes (PRCs), called PRC1 and PRC2/3/4.

Submitted December 25, 2009; accepted January 5, 2011. Prepublished online as *Blood* First Edition paper, February 2, 2011; DOI 10.1182/blood-2009-12-261602.

The online version of this article contains a data supplement.

The publication costs of this article were defrayed in part by page charge payment. Therefore, and solely to indicate this fact, this article is hereby marked "advertisement" in accordance with 18 USC section 1734.

© 2011 by The American Society of Hematology

This study shows a novel function of Evi1 to regulate the PTEN/AKT/mTOR signaling pathway and involvement of PRCs in PTEN down-regulation by Evi1. These results provide a possibility of overcoming the poor prognosis of patients with leukemia with high Evi1 expression, which is supported by our newly established mouse model and the analysis of human samples.

## Methods

### Subjects

Studies that involved human subjects were done in accordance with the ethical guidelines for biomedical research involving human subjects, which was developed by the Ministry of Health, Labor, and Welfare, Japan, the Ministry of Education, Culture, Sports, Science, and Technology, Japan, and the Ministry of Economy, Trade, and Industry, Japan, and enforced on March 29, 2001. This study was approved by ethical committee of Tokyo University. Written informed consent was obtained from all patients whose samples were collected after the guideline was enforced in accordance with the Declaration of Helsinki. All animal experiments were approved by the University of Tokyo Ethics Committee for Animal Experiments.

### Reporter assay

Analysis of luciferase activities was performed as described previously.<sup>8</sup> Briefly, cells were seeded in 12-well culture plates at a density of  $2 \times 10^4$ /well and were transfected with the use of FuGENE6 (Roche). The transfected cells were harvested 48 hours after transfection and assayed for luciferase activity with the use of dual luciferase kit (Piscagene). Firefly luciferase activity was measured as relative light units. The relative light units from individual transfection were normalized by measurement of Renilla luciferase activity in the same samples. Relative PTEN promoter activity was presented as the ratio of normalized luciferase activity of mock-transfected cells.

### Retrovirus production and bone marrow transplantation assays

These procedures were performed as described previously.<sup>1,33-35</sup> Briefly, Plat E packaging cells were transiently transfected with each retrovirus vector, and supernatant containing retrovirus was collected 48 hours after transfection and used immediately for infection. Fluorouracil-primed bone marrow (BM) cells isolated from C57/B6 mice were used for retroviral transduction. To establish Evi1-induced murine AML models, pMYs-Evi1-internal ribosome entry site (IRES)-green fluorescent protein (GFP) or empty retrovirus was used, and  $0.2-1.2 \times 10^6$  of Evi1-IRES-GFP<sup>35,36</sup> or GFP-transduced BM cells (Ly5.1) were injected through the tail vein into C57/B6 (Ly5.2)-recipient mice that had been administered a sublethal irradiation (5.25 Gy). To test the sensitivity of rapamycin *in vivo*,  $1 \times 10^6$  of Evi1-, translocated ets leukemia (TEL)/platelet-derived growth factor  $\beta$  receptor (PDGF $\beta$ R)-AML1/ETO-, or AML1\_S291fsX300-induced leukemic cells were injected to sublethally irradiated (7.5 Gy) secondary recipient mice. Diagnosis of AML was made according to the Bethesda proposals.<sup>37</sup>

### Colony-forming assays

For short hairpin RNA (shRNA)-mediated knockdown assays, transformed BM cells from the third to fourth round of *in vitro* replating were subsequently infected with retrovirus encoding shRNAs. After retroviral transduction, BM cells were resuspended in Methocult3434 (StemCell Technologies) at a concentration of  $4 \times 10^4$  cells/mL before selection or  $1 \times 10^4$  cells/mL after selection and seeded at 1 mL/35-mm petri dish in duplicate. Colony number of each dish was scored weekly. G418 (1.0 mg/mL) or puromycin (1.0  $\mu$ g/mL) was added to the Methocult for the purpose of selection. We defined a colony as a cluster of  $\geq 100$  cells. For *in vitro* inhibitor assays, rapamycin (Cell Signaling), LY294002 (Cell Signaling),

BMS345541 (Calbiochem), or DAPT (Calbiochem) was reconstituted with dimethyl sulfoxide (Sigma-Aldrich) and added to methylcellulose.

### siRNA interference

Specific siRNA oligos targeting EZH2, SUZ12, and EED mRNAs were designed as indicated by Clontech and cloned into pSIREN-RetroQ vectors. Control shRNA is a nonfunctional construct provided from Clontech. See supplemental Methods (available on the *Blood* Web site; see the Supplemental Materials link at the top of the online article) for more information.

### Quantitative real-time PCR

Real-time polymerase chain reaction (PCR) was carried out with the LightCycler480 (Roche) or the ABI PRISM 7000 Sequence Detection System (Applied Biosystems) according to the manufacturer's instructions. The results were normalized to  $\beta$ -actin levels. See supplemental Methods for more information.

### ChIP

Detailed protocols for chromatin immunoprecipitation (ChIP) assays are presented in supplemental Methods. Immunoprecipitated DNA fragments were quantified by real-time PCR with the use of the following primers (Figure 1D); PCR primers 1 and primers 3 amplify sequences, including putative Evi1 binding sites (5'-AGACAGGTGAGGAAA-3' fragment at position -4257/-4243 and 5'-AAAATAGAA-3' fragment at position 1935/1943, respectively), which were identified by the rVISTA2.0 tool (<http://rvista.dcode.org/>) with the use of a matrix similarity threshold of 0.80 and 0.85, respectively, and PCR primers 2 amplify a sequence, including possible murine Egr1 binding site (5'-CCGCCACTCGC-3' fragment at position -1907/-1896 upstream of the initiation codon ATG [+1]). Primers for human samples correspond to the primers 3 in Figure 1D, and they amplify a sequence, including 5'-AGAAGATAA-3' fragment.

### EMSA

Protein lysates were obtained from 293T cells transfected with plasmids encoding Flag-tagged Evi1 or its mutants, immunoprecipitated with EZview Red ANTI-FLAG M2 Affinity Gel (Sigma-Aldrich), and eluted with 3 $\times$  Flag peptide (Sigma-Aldrich) according to the manufacturer's recommendation. The procedures for electromobility shift assay (EMSA) were performed with the EMSA "Gel Shift" Kit (Panomics) according to the manufacturer's recommendation. Biotin-labeled probes were added. A competition control was set up by adding non-biotin-labeled cold probes to the reaction. See supplemental Methods for more information.

### Microarray analysis

Gene expression analysis was carried out as previously described<sup>1</sup> with the use of the Mouse Genome 430 2.0 Array (Affymetrix). All microarray data have been deposited in National Center for Biotechnology Information's Gene Expression Omnibus (<http://www.ncbi.nlm.nih.gov/geo/>) and are accessible through accession no. GSE22434. See supplemental Methods for more information.

### Statistical analysis

Statistical significance of differences between parameters was assessed with a 2-tailed unpaired *t* test. The correlation between Evi1 and PTEN expression was estimated with both the Pearson product-moment correlation coefficient and the Spearman rank-correlation coefficient. The overall survival of mice in BM transplantation assays was calculated according to the Kaplan-Meier method.

## Results

### PTEN is a direct target of Evi1

To identify new target genes of Evi1, we first carried out genomewide gene-expression analysis. BM cells derived from